RESEARCH ARTICLE

CrossMark

A tuff cone erupted under frozen-bed ice (northern Victoria Land, Antarctica): linking glaciovolcanic and cosmogenic nuclide data for ice sheet reconstructions

J. L. Smellie[1] · S. Rocchi[2] · J. S. Johnson[3] · G. Di Vincenzo[4] · J. M. Schaefer[5]

Abstract

The remains of a small volcanic centre are preserved on a thin bedrock ridge at Harrow Peaks, northern Victoria Land, Antarctica. The outcrop is interpreted as a monogenetic tuff cone relict formed by a hydrovolcanic (phreatomagmatic) eruption of mafic magma at 642 ± 20 ka (by ^{40}Ar-^{39}Ar), corresponding to the peak of the Marine Isotope Stage 16 (MIS16) glacial. Although extensively dissected and strewn with glacial erratics, the outcrop shows no evidence for erosion by ice. From interpretation of the lithofacies and eruptive mechanisms, the weight of the evidence suggests that eruptions took place under a cold-based (frozen-bed) ice sheet. This is the first time that a tuff cone erupted under cold ice has been described. The most distinctive feature of the lithofacies is the dominance of massive lapilli tuff rich in fine ash matrix and abraded lapilli. The lack of stratification is probably due to repeated eruption through a conduit blasted through the ice covering the vent. The ice thickness is uncertain but it might have been as little as 100 m and the preserved tephra accumulated mainly as a crater (or ice conduit) infill. The remainder of the tuff cone edifice was probably deposited supraglacially and underwent destruction by ice advection and, particularly, collapse during a younger interglacial. Dating using ^{10}Be cosmogenic exposure of granitoid basement erratics indicates that the erratics are unrelated to the eruptive period. The ^{10}Be ages suggest that the volcanic outcrop was most recently exposed by ice decay at c. 20.8 ± 0.8 ka (MIS2) and the associated ice was thicker than at 642 ka and probably polythermal rather than cold-based, which is normally assumed for the period.

Editorial responsibility: P-S Ross

Electronic supplementary material The online version of this article (https://doi.org/10.1007/s00445-017-1185-x) contains supplementary material, which is available to authorized users.

✉ J. L. Smellie
  jls55@le.ac.uk

1 Department of Geology, University of Leicester, Leicester LE1 7RH, UK

2 Dipartimento di Scienze della Terra, Università di Pisa, I-56126 Pisa, Italy

3 British Antarctic Survey, Cambridge CB3 0ET, UK

4 Consiglio Nazionale delle Ricerche, Istituto di Geoscienze e Georisorse, I-56127 Pisa, Italy

5 Lamont-Doherty Earth Observatory, Columbia University, New York, NY 10964, USA

Introduction

In glaciated terrains, the volcanic morphologies and lithofacies of the volcanic products are valuable indicators (proxies) for palaeo-ice type, thickness and extent (see Smellie and Edwards (2016) and Smellie (in press) for complete reviews). During the last 20 years, refinements to glaciovolcanic studies have enabled workers to establish the presence of ice, its age (mainly by ^{40}Ar-^{39}Ar dating), ice thickness and surface elevation, and ice basal thermal regime (e.g. Smellie and Skilling 1994; Edwards and Russell 2002; Schopka et al. 2006; McGarvie et al. 2007; Smellie et al. 2008, 2009, 2011a; Edwards et al. 2015). This is the largest range of critical parameters of past ice that can be obtained by any proxy methodology and, distinctively, many of these attributes are quantifiable (Edwards et al. 2015; Smellie and Edwards 2016; Smellie in press). Because of the wide

distribution of wet-based ice worldwide (e.g. Benn and Evans 1998) practically all of the published studies relate to eruptions in that setting (Smellie 2013; Smellie and Edwards 2016). By comparison, studies of volcanism under cold-based ice (also known as frozen-bed or polar ice) are rare and much remains to be determined. The few published studies have all involved effusive eruptions and the formation of 'a'a-sourced lava-fed deltas in Antarctica (Smellie et al. 2011a, b, 2014). The broad characteristics of eruptions under cold-based ice have also been treated theoretically (Smellie 2009, 2013), but there are no known published examples of volcanic sequences formed as a result of explosive eruptions under cold ice. Glacial thermal regime affects ice velocity, erosional and depositional rates (hence landforms), sediment loads, water chemistry, mass balance and the response time of ice to climate change and consequent effects on global sea levels (Benn and Evans 1998). The distinction between wet-based (i.e. relatively warm) and cold-based ice masses is thus important (e.g. Smellie et al. 2014). The physical properties of wet- and cold-based ice are also very different (summarised by Smellie 2009). Thus, being able to identify reliably the thermal regimes of past ice is important for palaeoenvironmental studies as well as for validating forward models of the effects of climate change (e.g. IPCC 2013).

In this paper, we describe the results of a linked glaciovolcanic–cosmogenic nuclide study of a volcanic outcrop in northern Victoria Land, Antarctica. We present a detailed description of the volcanic lithofacies and an ^{40}Ar-^{39}Ar age for the age of eruption. The environmental conditions prevailing during the eruptive period are also investigated and we provide a comprehensive model for the construction of a tuff cone in a cold-ice glacial setting. By describing the distinctive lithofacies characteristics of the resulting products, our study should increase and enhance the use of glaciovolcanism as a palaeo-ice sheet proxy. Because the outcrop is strongly dissected and overlain by numerous glacial erratics, we also obtained cosmogenic nuclide exposure ages for selected samples of the erratics. By linking the glaciovolcanic results to understanding the presence and significance of the erratics, an expanded much more holistic understanding of the outcrop is achieved, in particular its physical development and the morphological changes and thermal regime of the associated evolving ice cover.

Geological background

The geology of northern Victoria Land includes an extensive but poorly exposed tectonostratigraphical unit known as the Wilson Terrane (Stump 1995). The unit is composed of a Precambrian–Cambrian metasedimentary sequence and remnants of a granulite complex deformed during the Cambro–Ordovician Ross Orogeny (Stump

1995). It is intruded by a variety of plutons grouped together as the Cambro–Ordovician Granite Harbour Intrusive Complex which dominate the local outcrops (Nathan 1971; Carmignani et al. 1988; Rocchi et al. 1998, 2011). However, more recent studies have indicated that some of these plutons, with alkaline compositions, are of Cenozoic age (Rocchi et al. 2002). For example, syenites and monzonites are the main constituents of the Mt. McGee igneous complex and are found as dykes in the Styx Glacier area (Fig. 1; Tonarini et al. 1997). The plutons are mostly unfoliated and have mainly granite or granodiorite compositions. Harrow Peaks is largely formed by the Aviator Granite, a uniform biotite granodiorite. There are also small plutons of muscovite granite, biotite gabbro and diorite (Stump 1995). The Palaeozoic units are unconformably overlain across a major regional
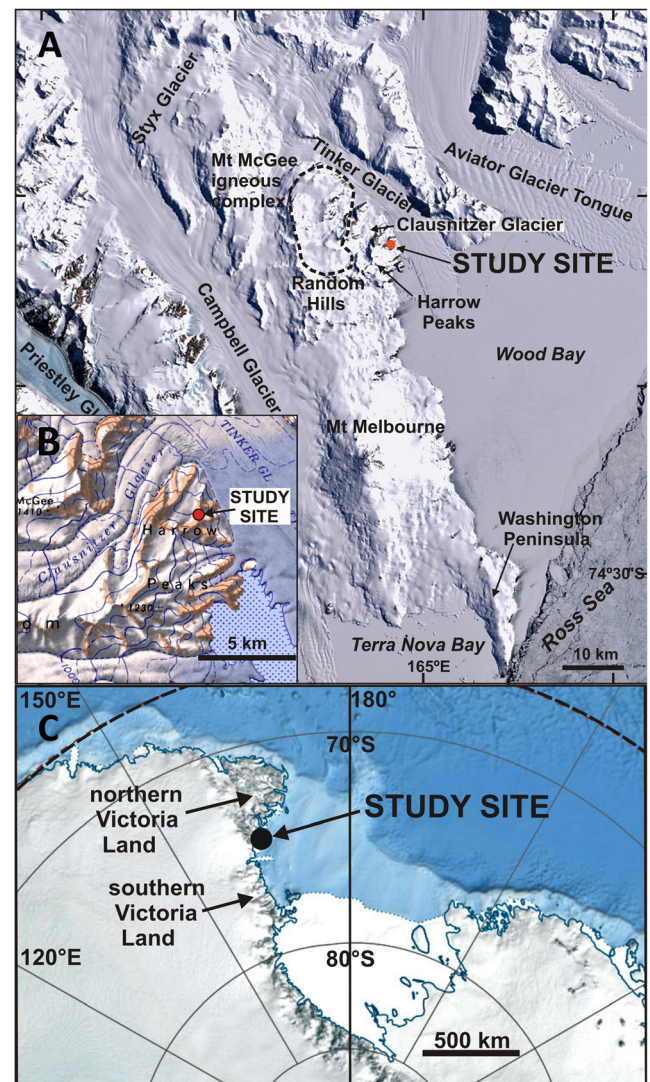

Fig. 1 Satellite images showing the location of the study area, Harrow Peaks, in northern Victoria Land, Antarctica, and localities mentioned in the text. Topographical base map used in B from USGS (1967)

unconformity known as the Kukri Peneplain by the Beacon Supergroup, an essentially flat-lying Permian–Lower Jurassic continental sedimentary sequence intruded by thick sills of the Lower Jurassic Ferrar Supergroup (Stump 1995). The Jurassic setting has been modified by the activity of the West Antarctic rift system (Rocchi et al. 2002). Cretaceous extension was followed by Cenozoic large-scale strike-slip faulting, coupled with Eocene–Oligocene intrusion of alkaline plutons and dykes and construction of volcanic edifices and volcanic fields all along the Ross Sea coast of Victoria Land since the Miocene (Salvini et al. 1997; Rocchi et al. 2002).

One of these volcanic edifices, Mt. Melbourne (2732 m a.s.l.), dominates a conspicuous promontory that separates Campbell Glacier from Wood Bay (Fig. 1). Mt. Melbourne is an active ice-clad volcanic stratocone 15 km in basal diameter that gives its name to the Miocene–Holocene Melbourne volcanic province and the mainly Plio–Pleistocene Mt. Melbourne volcanic field. The erupted magmas form a sodic alkaline magma association with compositions mainly ranging from alkali basalt to hawaiite, together with trachytes (Wörner et al. 1989; Armienti et al. 1991; Giordano et al. 2012). Its most recent eruption may have occurred between 1862 and 1922, based on the presence of tephra layers in ice cliffs on and close to the volcano (Lyon 1986). The undulating ice-covered foothills to the east and southeast of Mt. Melbourne are formed by the relics of several large Plio–Pleistocene volcanic shields (e.g. Washington Peninsula). Numerous small scoria and tuff cones are also scattered across the low-lying smooth Mt. Melbourne volcanic terrain (Wörner and Viereck 1987; Armienti et al. 1991; Giordano et al. 2012). The volcanic outcrop described in this paper is situated at Harrow Peaks (74° 03′ S, 164° 47′ E), a group of rugged peaks and ridges on the eastern flank of Random Hills overlooking Wood Bay (Fig. 1). Random Hills and Harrow Peaks contain several small scattered monogenetic scoria cones and lava outcrops belonging to the Mt. Melbourne volcanic field.

The Harrow Peaks study site is strongly eroded and dominated by a prominent central black basalt plug containing abundant peridotite nodules, basement xenoliths and mafic lower crustal nodules. The plug is surrounded by palagonitized lapilli tuff (Wörner and Viereck 1987; Giordano et al. 2012). Together, they represent a small tuff cone that was constructed on a narrow ridge crest in mid-Quaternary time. Although these previous workers considered that most of the volcanic outcrops in the Mt. Melbourne volcanic field were glaciovolcanic (i.e. erupted subglacially), very little supporting evidence has been published. Two additional centres that may be similar to that at Harrow Peaks occur to the south and north, but their details have not been described (Giordano et al. 2012).

Local topography and description of the study site

Harrow Peaks is bounded to the west by Random Hills, to the north and east by Tinker Glacier, and to the northwest by Clausnitzer Glacier (Fig. 1). Tinker Glacier is a large valley glacier with several tributaries, which flows into Wood Bay where it forms a prominent ice tongue at least 10 km long. Random Hills and Harrow Peaks are topographically similar, comprising icefields through which a relatively small amount of granitoid rock is exposed in several sharp-crested ridges. The intervening valleys are occupied by glaciers that, together with the ridges, form a dendritic pattern that is broadly radial to the local summit of Random Hills at 1770 m a.s.l. (Orombelli et al. 1990; Baroni et al. 2005); elevations in Harrow Peaks are much lower (below 1230 m and mainly below 1000 m). By contrast, the terrain surrounding Mt. Melbourne has a much smoother appearance and elevations are generally below 1000 m. The study site is situated on the saddle of one of the granitoid ridges on the north side of Harrow Peaks (Figs. 2 and 3). The volcanic outcrop extends from an elevation of c. 275 m a.s.l. at the base of the west side of the ridge, to c. 400 m a.s.l. at the outcrop summit.

Methodology

The field site was mapped during two separate visits on 11 December 2005 and 23 November 2011, when the major lithofacies were identified, sampled and described. Eleven volcanic rock samples were taken for thin section examination, whole-rock analysis and ^{40}Ar-^{39}Ar dating; two erratics were also sampled for cosmogenic dating. The vesicularity of juvenile sideromelane, clast sizes and proportions (including proportion of ash matrix) were estimated visually both in the field and under the microscope in selected representative specimens; the vesicularity is described in this paper using the categories of Houghton and Wilson (1989). Whole-rock analysis (for major elements) was determined by X-ray fluorescence (XRF-ARL 9400XP) at the Dipartimento di Scienze della Terra, Università di Pisa. Sample preparation and ^{40}Ar–^{39}Ar data collection were conducted at Istituto di Geoscienze e Georisorse, CNR, Pisa (methods described by Di Vincenzo et al. (2010). Preparation of the two erratics sampled for ^{10}Be exposure dating was carried out at Lamont-Doherty Earth Observatory cosmogenic nuclide laboratory using methods described by Schaefer et al. (2009). The erratics were located on and close to an exposed narrow ridge crest (Fig. 2) where surface gradients are much lower (10–30°) than on the ridge flanks (c. 50–70°), and they are slab-like. This combination should reduce the likelihood of post-depositional movement. We also think it is unlikely that snow cover of a considerable thickness (i.e. tens of centimetres) has

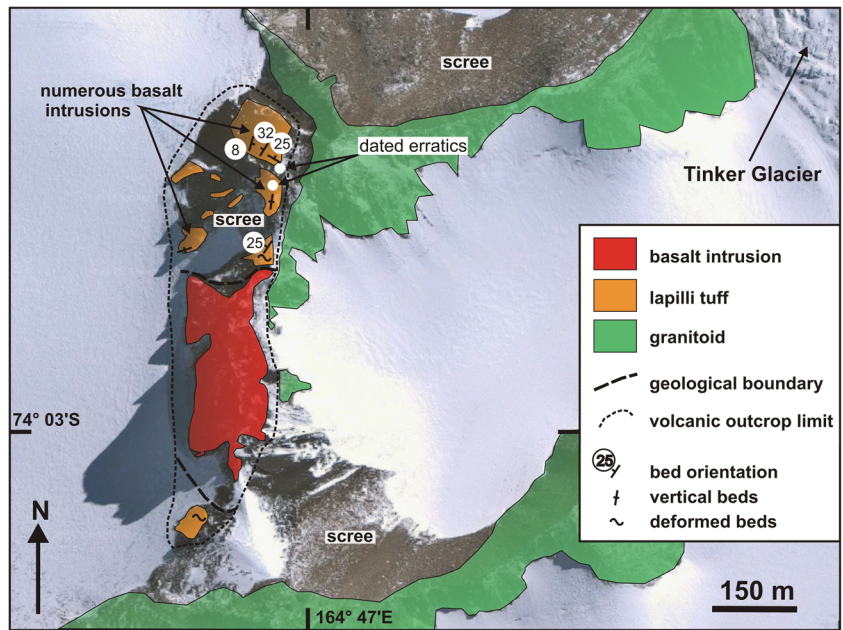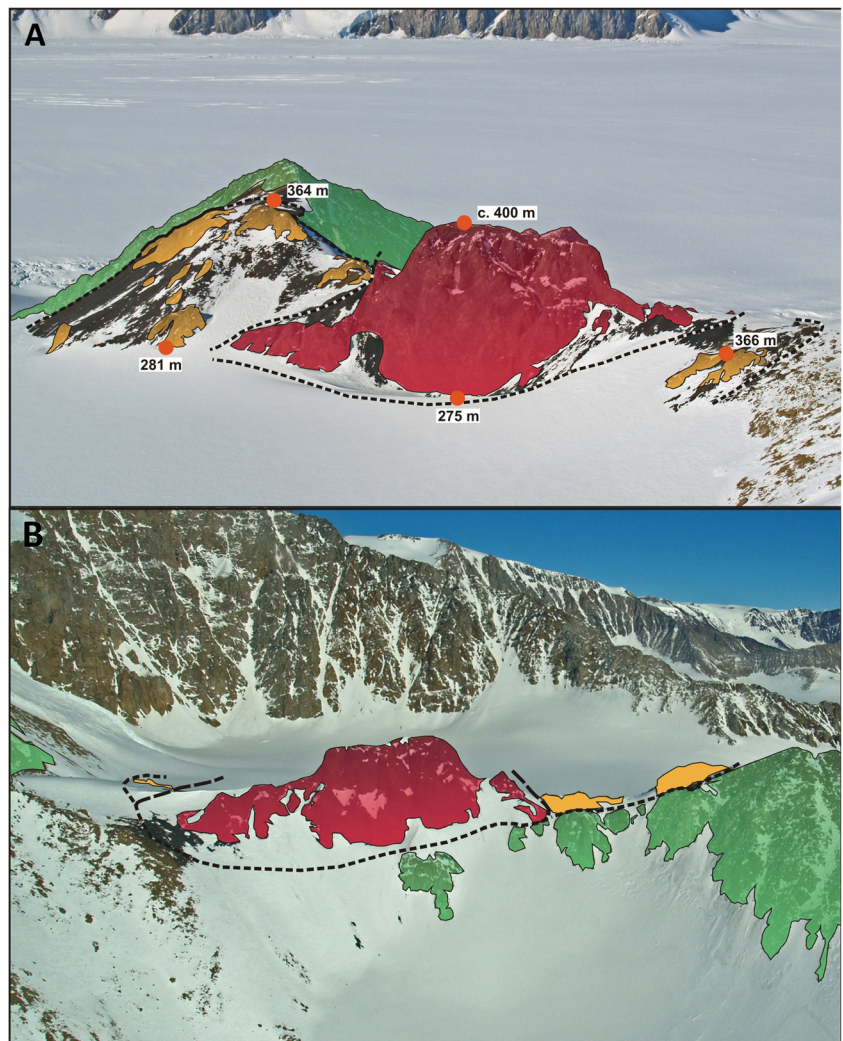**Fig. 2** Geological map of the study site at Harrow Peaks

Fig. 3 Aerial views of the study site at Harrow Peaks, with the geology and elevations measured by hand-held Garmin GPS altimeter shown. **a** View looking east, and **b** looking west, showing the much steeper slopes compared to (**a**)

episodically shielded the samples from cosmic radiation since deposition because it is a windy exposed location where snow accumulation (if any) would not last long. Both erratics are sub-angular in shape, and have a brownish weathered upper surface (Figs. S2 and S3 (in Supplementary Information)), from which the samples were collected using a hammer and chisel. Complete details of the whole-rock analysis and dating methods used are provided in Supplementary information. All elevations for the study site were determined by hand-held Garmin GPS instruments, one being a barometric combined altimeter with an estimated accuracy of better than 10 m; the barometric gps was calibrated at sea level (at least twice daily) at Mario Zuchelli Station, from where the study was conducted. Previous workers have suggested that the outcrops were much higher, c. 600–800 m a.s.l. (USGS 1967; Wörner and Viereck 1987; Giordano et al. 2012) but our measured elevations were reproduced within error on both GPS instruments during two separate visits, in 2005 and 2011, which suggests that they are accurate.

Petrology, field relationships and lithofacies of the Harrow Peaks volcanic outcrop

Lava at Harrow Peaks has a narrow compositional range comprising basanite to hawaiite, with total alkalis ($Na_2O + K_2O$) of 5.1–5.7 wt%, a Na_2O/K_2O ratio of 2.5 and normative *ne* 4.3–7.9 (Table 1). It is characterised by phenocrysts of abundant mainly small euhedral–anhedral olivine together with rare pale greyish-green clinopyroxene, large ragged anhedral

Table 1   Geochemical analyses of lava samples from Harrow Peaks

|	T5.5.4*	G 83**		T5.5.4	G 83
SiO2	45.51	46.59	Norms***		
TiO2	3.62	3.33	*or*	9.47	8.60
Al2O3	16.21	15.69	*ab*	19.75	22.98
Fe2O3T	14.52	13.39	*an*	21.30	22.27
MnO	0.19	0.19	*ne*	7.93	4.30
MgO	6.16	6.48	*di*	13.98	15.54
CaO	8.61	9.30	*ol*	16.58	15.84
Na2O	4.06	3.64	*mt*	2.51	2.32
K2O	1.60	1.45	*il*	6.88	6.35
P2O5	0.69	0.78	*ap*	1.60	1.81
LOI	− 0.15	− 0.74			
Total	101.02	100.10	classif.	Basanite	Hawaiite
			mg#	48.82	52.11

*This paper

**Giordano et al. (2012)

***Calculated assuming: (1) FeO3/FeO = 0.15

(2) total oxidation of Fe2+ on ignition

(3) analyses recalculated anhydrous

plagioclase and very rare euhedral brown amphibole. The groundmass is formed of pilotaxitic lathy plagioclase crystals, lesser intergranular olivine and tiny grains of opaque oxide.

The volcanic outcrops are draped unconformably on the saddle of a sharp-crested north–south-aligned ridge composed of Aviator Granite, and on the steep west- and east-facing slopes although the basal contact is not exposed (Figs. 2 and 3). The volcanic outcrop is extensively degraded and dominated by a high central boss c. 125 m high composed of dark grey basalt that forms a conspicuous plug-like feature. It is flanked to the north and south by patchy small outcrops of orange-brown lapilli tuff, which are better preserved on the west side of the ridge where the slopes are less steep (c. 50°) compared to the east flank (c. 70°). There are four principal lithofacies present, i.e. three fragmental (lapilli tuff, fine tuff, and scoria lapillistone/agglutinate) and one coherent (columnar basalt). Although the volcanic outcrop is the youngest geological unit observed in situ, the entire outcrop, including the summit of the central plug, is strewn with numerous large and small erratic blocks up to 1.5 m diameter composed of foliated and unfoliated granitoid rocks, including composite blocks of muscovite-biotite granite grading to schlieren migmatite, and rare smaller blocks of pink syenitic rocks (see Figs. S1–S3 in Supplementary information).

The dominant fragmental lithofacies consists of indurated massive to rarely diffusely stratified lapilli tuff (sensu Branney and Kokelaar 2002, and White and Houghton 2006) corresponding to LT and dsLT in the lithofacies notation of Smellie and Edwards (2016) (Fig. 4a–c). Size grading is present in some beds, but there is no clear sense of whether the grading is normal or reverse. Pale khaki yellow fine tuff is also present and forms a subordinate lithofacies (lithofacies T and dsT of Smellie and Edwards 2016). It is rare and beds are discontinuous and can only be traced for a few metres laterally. It differs from the lapilli tuff lithofacies principally in the absence of lapilli and most of the observations about the lapilli tuffs also apply. Bedding orientations are very variable over short distances (few metres to a few decametres) and include vertical stratification (Fig. 4c). Many outcrops have a very inhomogeneous texture comprising diffuse, ill-defined, better-sorted lapilli-rich domains enclosed in ash-rich lapilli tuff, and weather to a carious (i.e. decayed, pitted) appearance; they also include slabs of diffusely stratified lapilli tuff or fine tuff up to a few metres long, some of which show possible plastic deformation (Fig. 4a).

The lapilli tuff deposits are composed of abundant brownish-yellow sideromelane ash and lapilli generally ≤ 5 mm in diameter, ranging up to 3 cm, with blocky angular shapes and variable vesicularity (mainly moderately to poorly vesicular; more rarely non-vesicular or highly vesicular; Figs. 4b and 5a). The sideromelane contains abundant aligned plagioclase microlites and is unaltered but for a narrow rim of fibro-palagonite, and some vesicles contain fibrous zeolite.

Fig. 4 Views of the volcaniclastic lithofacies. **a** Massive lapilli tuff. This is the typical lithofacies in the tephra outcrops. Note the inhomogeneous carious texture of the outcrop at left, caused by variable weathering of ill-defined patches or domains of lapilli-rich and ash-rich tephra, and the diffuse-margined slab of stratified lapilli tuff; the hammer is 50 cm long. **b** Close view of typical massive lapilli tuff lithofacies; the pencil is 8 cm long. **c** Vertical stratification in diffusely stratified lapilli tuffs. **d** Lens of ash-coated lapilli within lapilli tuff. **e** Stratified scoria lapillistones resting on massive lapilli tuff, both intruded by prismatic jointed mafic lava. Note the blocks of white granitoid contained in both the scoria lapillistone and the basalt plug (above figure and upper left side). **f** Close view of dark grey lapillistone showing coarse scoria and ragged slightly flattened bombs; the pencil is 13 cm long
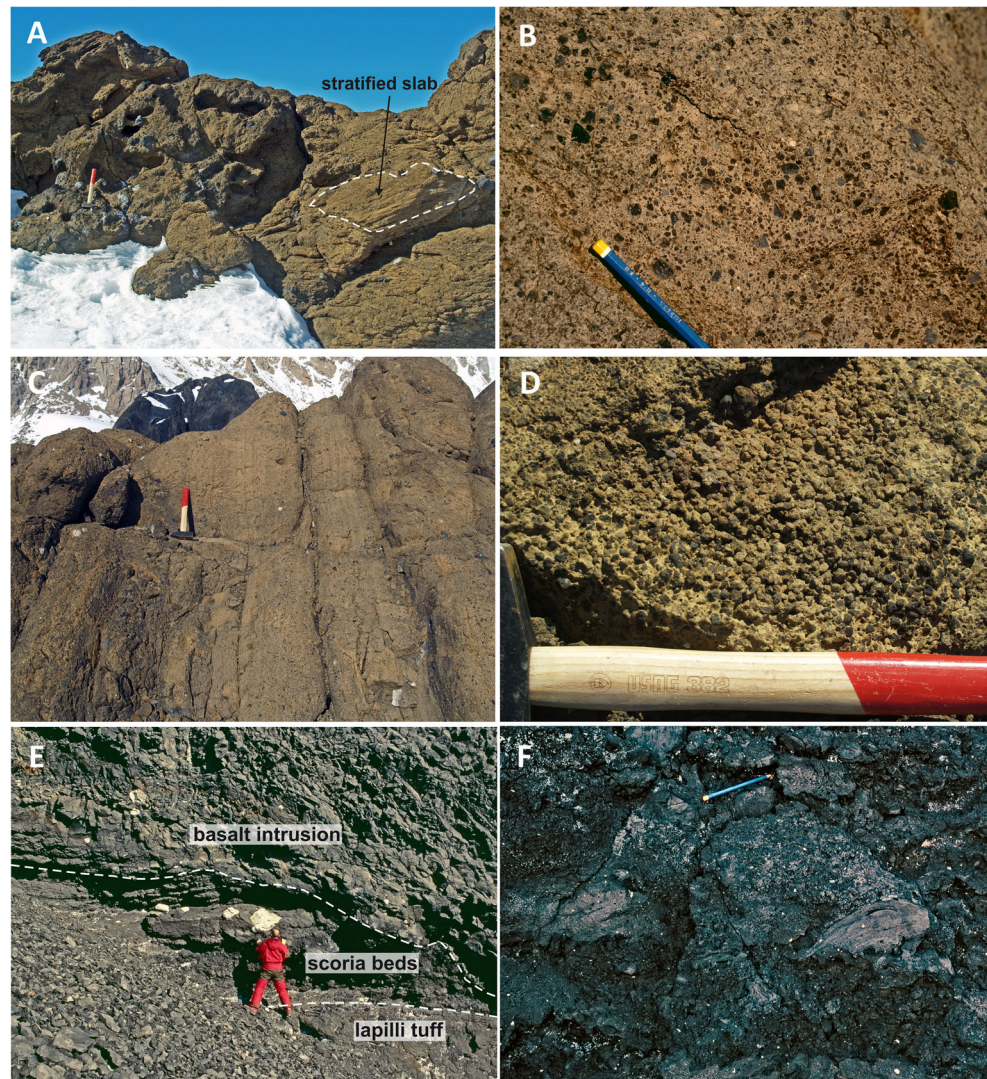
Tachylite lapilli are also present but form < 10 vol%; they occasionally occur within sideromelane lapilli (Fig. 5c). Many tachylite and sideromelane lapilli show signs of abrasion. There are impersistent ill-defined lenses a few centimetres thick dominated by relatively well sorted lapilli 1–3 cm in diameter and just 20 vol% ash matrix; some of the latter lenses are dominated by ash-coated lapilli (cored ash pellets, sensu Brown et al. 2012; Fig. 4d). The mineral assemblage in the sideromelane and tachylite resembles that of the basalt neck, with abundant small euhedral–anhedral olivine phenocrysts, rare anhedral greyish green clinopyroxene, and occasional large partially resorbed anhedral plagioclase phenocrysts; brown biotite and muscovite xenocrysts are also rarely present. Fine to coarse ash matrix is generally abundant (c. 30–60 vol%) and is noticeably rich in the fine ash component (Fig. 5). It is formed of blocky incipiently to non-vesicular sideromelane (Fig. 5a) but the finest grains are often pervasively clay altered (palagonite). Vesicles are rarely present in the matrix (Fig. 5b). Ragged to rarely spherical grey

juvenile bombs up to 50 cm across (usually < 20 cm) are uncommon and form c. 1% of the rock. Some bombs are cored by granitoid blocks. Dispersed blocks of white granitoid, some foliated, and fewer pink syenitic rocks also form c. 1% of the rock. The blocks are up to 70 cm across (usually < 10 cm) and have angular–subangular or rarely sub-rounded shapes. Giordano et al. (2012) suggested that the lower beds are richer in granitoid lithic clasts, but we were unable to confirm the observation.

Dark grey scoria lapillistone and agglutinate occur only within the central plug outcrop as patches, screens and slabs. The screens and slabs are a few to 10 m thick, up to a few tens of metres long, and intruded by basalt. The lithofacies is composed of glassy highly vesicular scoria and ragged juvenile bombs (Fig. 4f). At some locations the bombs are abundant, flattened parallel to bedding and welded (i.e. agglutinate). Bombs are typically a few decimetres across and highly and coarsely vesicular. Spindle, ropy-textured ribbons and cowpat varieties are present, together with rare decimetre-size dense
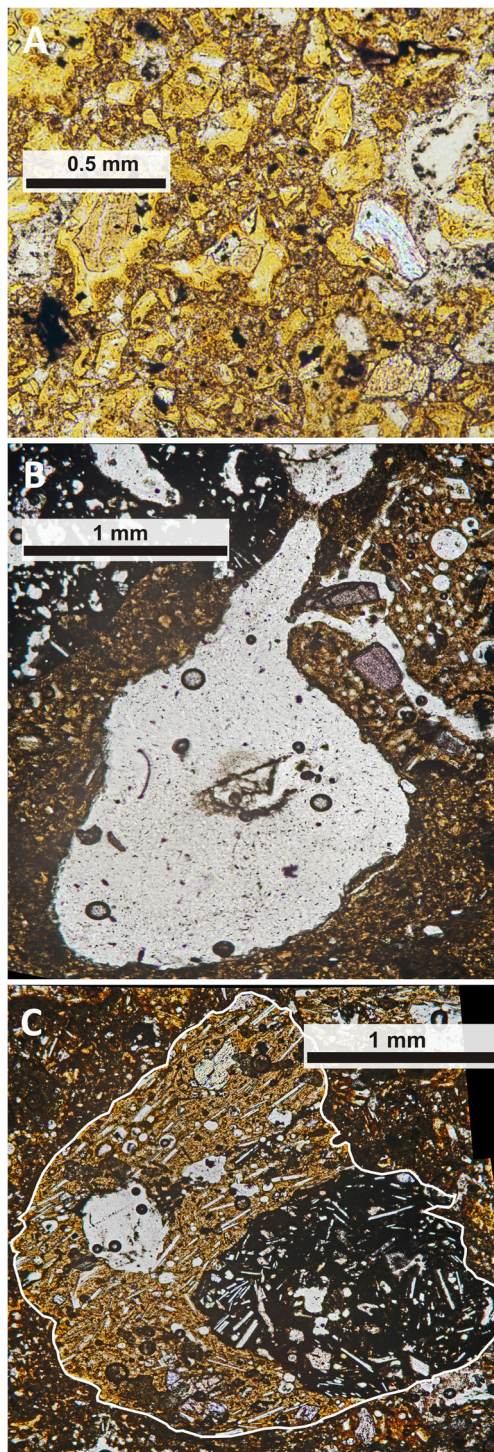
Fig. 5 Photomicrographs of Harrow Peaks lapilli tuffs. **a** Fine–medium ash matrix to lapilli tuff showing blocky sideromelane shapes. **b** Matrix vesicle in fine ash matrix of lapilli tuff. **c** Abraded tachylite clast within sideromelane lapillus

lava balls and dense ribbon bombs up to 3 m long and 20 cm thick. The lithofacies is composed of dark brown to blackish oxidised scoria and bombs petrologically similar to those in the lapilli tuffs and containing conspicuous but minor (<

1 vol%) white granitoid blocks similar to those in the lapilli tuffs. Crude planar stratification is present and was observed resting conformably on massive lapilli tuff (Fig. 4e). Contacts with the plug are both sharp and gradational, with basalt of the plug becoming more closely jointed, then jigsaw jointed and brecciated before passing out into scoria.

The coherent lithofacies is columnar basalt. It is dark grey and forms the prominent central plug-like mass and numerous small irregular and sheet-like intrusions in the northern lapilli tuff outcrops. This basaltic mass measures approximately 400 m north to south, 150 m west to east and is well exposed in sheer rock faces 100–125 m high (Figs. 2 and 3). It is composed of pervasively columnar-jointed rock. The contact with the surrounding lapilli tuffs is unexposed but the basalt intrudes both lapilli tuff and scoria/agglutinate lithofacies (Fig. 4e). The columns are predominantly narrow, with diameters mainly c. 15–25 cm but increasing locally to 40–60 cm. On top surfaces they resemble blocky jointing (Fig. 6a). Column attitudes are very variable and curved, and diverging-fan patterns are common (Fig. 6b). They locally give the appearance of large-scale, but irregular, lava lobes several tens of metres in length and were called megapillows by previous workers (Wörner and Viereck 1987; Giordano et al. 2012). However, no glassy chilled internal surfaces were seen, and boundaries are merely finer grained and appear to be gradational rather than abrupt. The lava is finely crystalline (pale grey) to aphanitic (dark grey).

Numerous irregular to sheet-like masses of columnar basalt with variable attitudes (dyke- and sill-like) intrude the northern lapilli tuff outcrop. They are petrologically similar to the basalt forming the plug. The intrusions are up to c. 7 m in width but are usually just 2–4 m wide, and they can be traced for a few tens of metres. Most are irregular in shape with sinuous or bulbous margins resembling incipient pillows (Fig. 6c). Several have cm-thick glassy chilled margins but others have margins of aphanitic basalt up to 10 cm thick. They are patchily vesicular. The vesicles are usually sparse (c. 10–15%) and small (few millimetres, up to c. 3 cm) but some parts are frothy and locally they contain distinctive large vesicles up to 10 cm in diameter that have smooth fluidal internal surfaces. Like the plug outcrop, the tone varies according to the crystal size and they are relatively coarsely columnar and blocky jointed (joints spaced at c. 20–35 cm). The intrusions have rarely baked the adjacent lapilli tuffs in zones up to 40 or 50 cm wide in which the sideromelane is deep reddish brown to sub-opaque in thin section. Ash-size matrix in the baked lapilli tuffs is relatively minor, typically 20–40 vol%, and lacks palagonite alteration or zeolites. In places, a discontinuous zone of laminated fine to coarse tuff up to 20 cm wide intervenes between the intrusion and the baked lapilli tuffs, with the laminations steeply-dipping parallel to the intrusion surface (Fig. 6d).
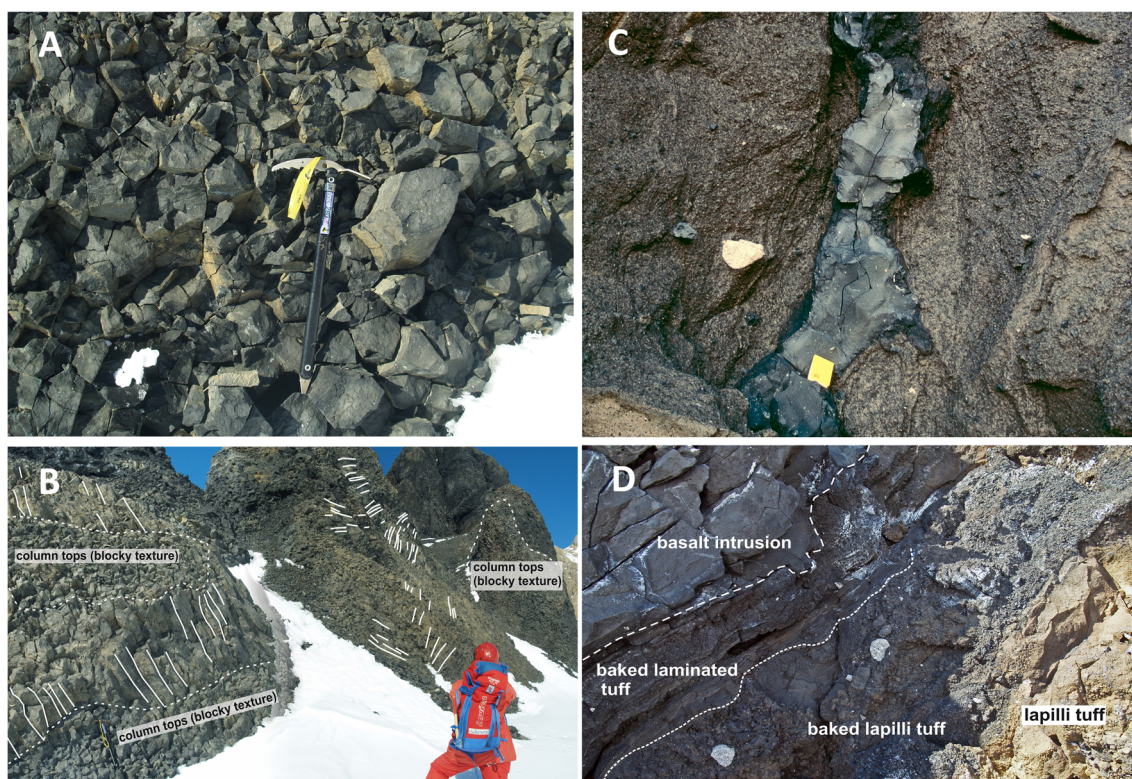
Fig. 6 Views of the coherent lithofacies. **a** Blocky jointing in the basalt plug; the ice axe is 60 cm long. **b** Entablature (also known as kubbaberg) prismatic jointing in the basalt plug; selected prismatic joints shown by white lines to highlight orientation variations. **c** Thin dyke intruding massive lapilli tuffs showing sinuous shape; the dyke has cm-thick glassy margins. The notebook is 17 cm long. **d** Prismatic-jointed sheet intrusion flanked by a 50 cm-wide zone of baked dark grey massive lapilli tuff; a 20 cm-wide zone of steep-dipping laminated tuffs intervenes

Geochronological framework

Age of the Harrow Peaks volcanic complex

A ^{40}Ar-^{39}Ar isochron age of 669 ± 101 ka and a preferred mean age of 745 ± 66 ka were published by Giordano et al. (2012), with high uncertainties, for olivine- and plagioclase-bearing black basalt from the central columnar plug at Harrow Peaks. Results were reported for furnace step-heating experiments from five whole-rock aliquots. All five runs were characterised by low radiogenic Ar contents (^{40}Ar* within 5–15% for more than 80% of the total heating steps) and, as a consequence, by step ages with large uncertainties (2σ analytical errors on step ages $> 7.7\%$, and $> 20\%$ for more than 50% of the total heating steps).

To better constrain the age, we selected a sample of fresh basalt from the central plug. The results are summarised in Table 2 and indicate an age of 642 ± 20 ka (also see Supplementary Information). Step-heating results are presented in Fig. 7. The age spectrum is internally discordant, with an overall descending shape. Four consecutive steps from the intermediate temperature region, representing more than 50% of the total $^{39}Ar_K$ released and characterised by the highest radiogenic Ar contents (^{40}Ar* 37–45%), define a concordant segment (MSWD = 0.98) with an error-weighted mean age of 642 ± 20 ka, indistinguishable at the 2σ level from the total gas age (616 ± 20 ka).

The step ages from our results largely overlap at the 2σ level (analytical errors) with those obtained by Giordano et al. (2012), even if their data seem to suggest a slightly older age (their preferred mean age is 745 ± 66 ka). The reason for the difference is uncertain although we suspect that the basalt analysed by Giordano et al. (2012) was less pristine than our sample. Based on the higher radiogenic Ar contents of our results, we suggest that the age of eruptions that formed the Harrow Peaks volcanic outcrop is c. 640 ka.

Exposure age of erratics overlying the Harrow Peaks volcanic outcrop

Numerous erratics are strewn across the volcanic outcrop, including on the narrow summit of the basalt plug (Fig. S1 (Supplementary Information)). Two of the larger basement erratics—measuring $95 \times 50 \times 45$ cm and $130 \times 110 \times 65$ cm respectively—overlying lapilli tuff outcrops were sampled for surface exposure dating.

We obtained ^{10}Be exposure ages from each of the erratics to determine when ice last covered the volcanic outcrop. They provide an important first-order constraint on ice sheet decay at Harrow Peaks, about which little is currently

Table 2 New ^{40}Ar-^{39}Ar data for a sample of the basanite plug at Harrow Peaks*

Sample number (PNRA)	Sample number (BAS)	Locality	Remarks	Total gas age (ka)	±2 s (internal error; ka)	Weighted mean age (ka)	±2 s (internal error; ka)	total # of steps or analyses	# of steps or analyses used in the weighted mean calculation	^{39}Ar$_K$ %
11.12. 05JS4	T5.5.4	Harrow Hills (74°02.8'S 164°47.46′ E)	Basalt neck cutting lapilli tuffs of tuff cone outcrop	616	20	642	20	9	4	51.4

Material analysed—groundmass; Technique—laser step-heating analysis (Nd-TAG laser); For full dataset, see Table S1 (Supplementary Information)

known. Sample information and summary ^{10}Be age data are shown in Table 3.

The presence of erratics perched on bedrock at 368 m above sea level at Harrow Peaks indicates that ice covered this site at some time in the past. Our two erratic samples yielded ^{10}Be exposure ages of 22.9 ± 0.8 and 18.7 ± 0.7 ka. We do not think that the younger age (18.7 ka) could be anomalously young, because the erratics are both large, have intact upper surfaces and are perched in stable positions. Therefore their exposure ages are unlikely to reflect snow cover, post-depositional erosion or post-depositional movement. Nevertheless, we cannot rule out the possibility that the 22.9 ka age is anomalously old, perhaps reflecting some inheritance of ^{10}Be from exposure to cosmic radiation during a previous ice-free period. This is a common problem in Antarctica because erosion rates are typically low, with the result that cosmogenic nuclides that accumulated in the surface of erratics prior to the last glaciation are not always completely eroded during glacial transport and may therefore contribute to the concentration measured; see

Fig. 7 ^{40}Ar-^{39}Ar plateau diagram showing the age of the central plug in the Harrow Peaks outcrop. Results for five replicates published by Giordano et al. (2012) are also shown for comparison (background, in blue)

Balco (2011) for further explanation. We therefore choose to take the mean of these two ages (20.8 ± 0.8 ka) to represent the most likely timing of deglaciation of this site.

Discussion

Style of eruption at Harrow Peaks

The abundance of sideromelane, palagonite alteration, high proportion of fine ash and the variable but generally moderate–low vesicularity of the juvenile lapilli and their blocky angular shapes indicate that the lapilli tuffs at Harrow Peaks are a product of explosive hydrovolcanic (phreatomagmatic) eruptions. Monogenetic edifices created by phreatomagmatic eruptions are either tuff cones, tuff rings or maars (Wohletz and Sheridan 1983). No primary landform is preserved at Harrow Peaks. However, the very low proportion of bedrock lithics and the abundant evidence for wet conditions (see below) suggest that the magma passed quickly and efficiently to the surface, with explosions rapidly confined to within a volcanic construct that was probably water saturated (Sohn 1996; White 1996). The conditions are most similar to those that construct tuff cones, with their abundant water sourced from surface water or a free-flowing aquifer, rather than either tuff rings or maars, with their less efficient delivery of groundwater-sourced water (cf. Wohletz and Sheridan 1983; Verwoerd and Chevalier 1987; Sohn 1996; White and Ross 2011).

The rare presence of matrix vesicles attests to the expansion of a gas phase trapped in a moist fine ash-rich host (Lorenz 1974). Although they are common in pyroclastic density current deposits, the water involved in the matrix vesicles at Harrow Peaks may have been transformed to steam from heat transmitted to the lapilli tuff pile by the numerous associated intrusions. The poorly preserved diffuse planar stratification lacking impact structures is typical for deposits of fully dilute pyroclastic density currents (sensu Branney and Kokelaar 2002), and wet pyroclastic currents carry abundant fine-grained material (Walker 1984), as is noted here for the
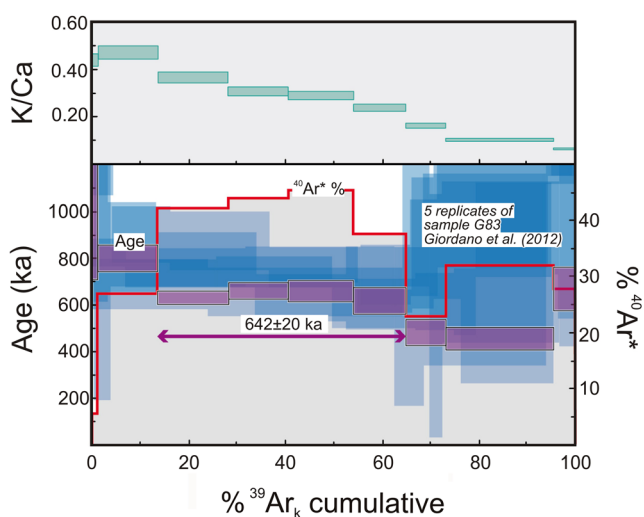
Table 3 Summary of cosmogenic nuclide exposure ages on basement erratic blocks from Harrow Peaks*

Sample	Latitude (S)	Longitude (E)	Altitude (m a.s.l.)	^{10}Be conc. (at g^{-1})	1σ error (at g^{-1})	^{10}Be age* (year)	1σ error* (year)	1σ propagated error** (year)
T11.8.1	− 74.04755	164.79062	363	158602	2958	22,900	400	800
T11.8.2	− 74.04735	164.79093	357	126882	2911	18,700	400	700

*Rounded to nearest 100 years

**Error propagated with production rate uncertainty of 2.3% (Putnam et al. 2010)

*See also Table S2 (Supplementary Information)

Harrow Peaks deposits. The presence of ash-coated juvenile lapilli also attests to formation within a moist ash-rich subaerial eruption column similar to the formation of ash aggregates (e.g. Brown et al. 2012). Deposition of the ash-coated lapilli may have been directly as fall layers, now disrupted, or they were incorporated into moving pyroclastic density currents, although in the latter situation they would be expected to transform into cored accretionary lapilli (Brown et al. 2012). The relatively abundant granitoid clasts present at the base of the sequence, some of which are noticeably abraded, may be rip up clasts incorporated into a mass flow unrelated to explosive interaction with groundwater (G. Giordano, personal communication, 2017). However, we did not observe the deposits described by Giordano et al. (2012) and a pyroclastic origin may also be feasible, following initial thermohydraulic explosions sourced within the bedrock (Wohletz and Sheridan 1983). The pervasive narrow-diameter curvicolumnar and blocky jointing seen in the coherent lithofacies resembles entablature, also known as kubbaberg (Sæmundsson 1970; Long and Wood 1986). The development of entablature indicates rapid lava cooling in a damp or wet milieu, and the irregular shapes of the associated intrusions within lapilli tuff, some with bulbous margins and glassy surfaces locally resembling incipient lava pillows, also suggest intrusion into a wet or damp unconsolidated tephra pile. Finally, the mega-vesicles present in some of the basalt intrusions may signify incorporation of trapped external water, and the zones of laminated tuffs at the margins of some intrusions are probably an effect of gas (steam) streaming causing localised fluidisation of adjacent unconsolidated wet or damp tephra. Conversely, the presence of more coarsely spaced (up to 35 cm) columnar joints in some of the intrusions, thick chilled margins that are fine grained rather than glassy, and the baking of adjacent lapilli tuffs to become oxidised (rather than pervasively palagonite altered) suggest slower cooling in somewhat drier deposits. A range of water conditions is therefore suggested by the evidence. Moist to wet conditions were probably prevalent until the vent dried out at a late stage.

The general absence of bedding or stratification in the overwhelmingly massive Harrow Peaks tephra pile is unusual. It is the most distinctive feature of the tephra outcrop and contrasts with both subaerial and subaqueous tuff cones, which are characteristically well stratified (e.g. Sohn 1996; White 1996; Cole et al. 2001; Smellie 2001; Schopka et al. 2006; Solgevik et al. 2007; Brand and Clarke 2009; Sohn et al. 2012; Russell et al. 2013; Table 4). Poorly sorted massive deposits in pyroclastic cones occur in beds deposited from granular fluid-based currents (Branney and Kokelaar 2002). Although such an origin might plausibly explain how much of the tephra was formed, the Harrow Peaks deposits are not bedded and their modes of transport and deposition are therefore uncertain but interpreted here as deposits of pyroclastic density currents. However, there is evidence that at least some of the tephra pile was stratified initially and the bedding was subsequently destroyed. This is suggested by the following: the highly variable orientations of the rare stratification present, which includes vertical beds (Figs. 1 and 4c); the presence of detached slabs of stratified lapilli tuff and fine tuff (Fig. 4a), some showing possible ductile folding; and ill-defined diffuse decimetre-scale patches, or domains, of better-sorted lapilli-rich rock within ash-rich lapilli tuff host that may be explained as the disruption and partial homogenization of a variably but poorly consolidated stratified pile (cf. Smellie et al. 2016). Similar bedded pyroclastic megablocks commonly occur within non-bedded volcanic hosts in the lower, unbedded parts of diatremes together with ill-defined diffuse decimetre-scale patches or domains of better-sorted lapilli-rich rock within ash-rich lapilli tuff (White and Ross 2011; and personal communication from P.-S. Ross, 2017).

Two principal processes can be envisaged for the destruction of original stratification: (1) repeated sector collapses followed by transport and redeposition as multiple mass flows; and (2) large-scale explosive mixing and reworking within the vent and associated crater. Method (1) is less plausible because it is likely to form identifiable thick beds (mass flow deposits) and therefore some stratification albeit probably coarse, which are not seen. Moreover, because the present tephra outcrop forms a narrow zone extending just 300 m beyond the basalt plug, it is vent proximal and probably represents mainly a crater or conduit fill. Some support for this suggestion comes from the presence of abraded juvenile lapilli and the high content of fine ash in the lapilli tuffs. Lapilli abrasion can occur during transport in pyroclastic density currents and much of the abrasion takes place relatively

Table 4 Geological attributes of mafic tuff cones erupted in different environmental settings

Environmental setting	Thermal regime	Ice thickness[3]	Dominant fragmental lithofacies	Subordinate fragmental lithofacies	Coherent lithofacies	Stratification	Deformation, internal discordances	Aspect ratio of preserved volcanic edifice[4]	Examples
1. Glaciovolcanic	Wet-based[1]	Thin	Stratified lapilli tuff; scoria breccia; agglutinate; possibly abundant basement lithics	Tuff; tillite; fluvial sediments	Intrusions	Well developed throughout, conspicuous; low angle dips at high elevations in tuff cone	Common, conspicuous, range of scales (single bed to large-scale sector collapse); prominent slump scars	Moderate; steep flanks with shallow-dipping bedding at high elevation	Deception Island 1969 & Icefall Nunatak, Antarctica (Smellie 2001, 2002)
	Wet-based[1]	Thick	Stratified lapilli tuff; possibly abundant basement lithics in basal beds	Tuff; scoria breccia; agglutinate; tillite; fluvial sediments	Intrusions; pillow lava	Well developed throughout, conspicuous; low angle dips at high elevations in tuff cone	Common, conspicuous, range of scales (single bed to large-scale sector collapse); prominent slump scars	Moderate; steep flanks with shallow-dipping bedding at high elevation	Helgafell, Breknafjoll & Herdubreidartogl, Iceland (Werner and Schmincke 1999; Schopka et al. 2006; Bennett et al. 2009)
	Cold-based[2]	Thin	Massive lapilli tuff; scoria breccia; agglutinate; possibly abundant basement lithics in basal beds	Tuff	Intrusions	Minor or not present at all	Pervasive but deposits largely disrupted (homogenised) and not conspicuous	High but significantly modified by sector collapse caused by ice decay	Harrow Peaks [THIS PAPER]
	Cold-based[2]	Thick	Massive lapilli tuff; possibly abundant basement lithics in basal beds	Tuff; possibly scoria breccia & agglutinate	Intrusions; pillow lava	Minor or not present at all	Pervasive but deposits largely disrupted (homogenised) and not conspicuous	High but significantly modified by sector collapse caused by ice decay	None known, characteristics inferred here
2. Subaerial (interaction with groundwater)	n/a	n/a	Stratified lapilli tuff with abundant basement lithics	Tuff; scoria breccia; agglutinate; palaeosols	Intrusions	Well developed throughout, conspicuous; parallel to cone surface, becoming asymptotic to base	Present, but generally inconspicuous	Low; flanks at or close to angle of repose	Korea (Sohn 1996; Sohn et al. 2012; Varda, Iceland (Smellie et al. 2016)
3. Subaqueous (lacustrine, marine)	n/a	n/a	Stratified lapilli tuff	Tuff; scoria breccia; agglutinate; fossils	Intrusions; pillow lava[5]	Well developed throughout, conspicuous; parallel to cone surface, becoming asymptotic to base	Present, including slump scar surfaces, but not common or conspicuous; may include beach deposits due to wave action	Low; flanks at or close to angle of repose	Korea (Sohn 1996; Sohn et al. 2012); Pahvant Butte, Table Rock, USA (White 1996; Brand and Clarke 2009); Surtsey (Kokelaar 1983; Moore 1985); Capelhinos, Azores (Cole et al. 2001; Solgevik et al. 2007)

[1] Includes warm ('temperate') & polythermal ice

[2] Also known as frozen-bed or 'polar'

[3] Thin =< c. 150 m; thick => c. 150 m (after Smellie and Skilling 1994)

[4] Aspect ratio: edifice height divided by basal diameter (after Smellie 2013); pristine edifices only

[5] In shallow water, eruptions will be explosive throughout and lack pillow lava

proximally, but a few *kilometres* of travel is required (Houghton and Smith 1993; Manga et al. 2011). The Harrow Peaks deposits are demonstrably proximal and lateral transport was minimal (few hundred metres at most), and only minor abrasion would be expected. Therefore, we suggest that the abrasion shown by many of the juvenile lapilli was probably caused by multiple cycles of reworking within the vent. In this scenario, clasts would be ejected vertically, perhaps in a water-rich, dense and relatively low column, before falling back into the crater only to be ejected again, repeatedly (Cioni et al. 2014; D'Oriano et al. 2014). This suggestion is supported by the presence of rounded juvenile tachylite lapilli, which probably record heating and abrasion in the vent during recycling (D'Oriano et al. 2014). The occurrence of abraded tachylite occurring within sideromelane lapilli (Fig. 5c) is also unequivocal evidence for clast recycling. Abrasion and comminution during abundant clast collisions in the vent and in turbulent eruption columns would also contribute to the high proportion of fine ash present (Kokelaar 1983; Rose and Durant 2009).

The occurrence of scoria lapillistone and agglutinate with large juvenile bombs up to 3 m long is also consistent with the fragmental deposits being vent proximal. Their presence corresponds to Strombolian activity and normally taken as an indication that the vent dried out at a late stage in the eruption, with the construction of a small scoria cone probably within the tuff cone crater (cf. Sohn 1996; Cole et al. 2001; Solgevik et al. 2007). At that stage, the explosions were less violent and they were driven by the escape of juvenile volatiles contained in the magma. However, an alternative explanation might be that the magma discharge rate increased, thus transforming the eruptive style from phreatomagmatic to magmatic (Valentine and White 2012). This suggestion is consistent with the models for tuff cone and tuff ring evolution described by Sohn (1996, his Fig. 4). The scoria cone itself was ultimately completely removed at the study site, probably by edifice collapse (see below), but relicts that subsided into the conduit are preserved as screens and slabs in the central plug.

The final eruptive episode involved the emplacement of a substantial plug-like mass of largely degassed basalt in the core of the lapilli tuff pile, together with numerous smaller satellite intrusions injected into the surrounding lapilli tuffs. The pervasive prismatic joints interpreted as entablature together with blocky cooling joints and the bulbous to incipiently pillowed margins of some of the intrusions indicate that emplacement occurred while the tephra was still unconsolidated and moist or wet. The large-scale (several decametres extent) poorly defined lobe-like structures in the plug, with ill-defined margins indicated by the complicated prismatic joint patterns, suggest that the plug might have been emplaced in multiple closely spaced stages. The structures were called megapillows by Wörner and Viereck (1987) and Giordano et al. (2012) and were used as evidence to suggest a broad

subglacial setting for the outcrop. Their presence argues against the en masse emplacement of the plug in a single intrusive event. However, the surfaces between the lobes are relatively diffuse with no sharp contacts and they are very fine grained rather than glassy. Thus, an alternative simpler explanation is that the very varied column orientations are simply a consequence of a chaotic cooling regime affecting the isotherms in a single large basalt mass and caused by the penetration of water along the column joints (Long and Wood 1986). Regardless of which explanation is correct, the central plug was emplaced within unconsolidated volcaniclastic rocks. The massive ash-rich lapilli tuffs, in the moist part of the pile at least, probably deformed pseudoplastically because of the high fine-ash content and surface tension forces imparted by water menisci acting to bind the grains, similar to cohesive forces acting in subaerial debris flows (Mulder and Alexander 2001).

Eruptive palaeoenvironment of the Harrow Peaks tuff cone

The water involved in the Harrow Peaks eruptions is unlikely to have been marine. The Harrow Peaks tuff cone is situated c. 2 km inland from Wood Bay (or rather, the Tinker Glacier valley leading into Wood Bay) and its vent was situated on a ridge crest at c. 350 m a.s.l. Studies of raised beaches in the Terra Nova Bay region have shown that late Quaternary uplift is minimal (< 30 m; Baroni and Orombelli 1987; Orombelli et al. 1990). Moreover, if glacial conditions prevailed, coeval sea level would be lower. In addition, a grounded Tinker Glacier would have occupied its valley and any seawater would have been displaced a few more kilometres further away. Therefore, the deposits are probably too far inland and the vent elevation too high for magma interaction to have occurred with seawater. A pluvial lake is also unlikely. With the young outcrop age, the present topography is probably similar to that at 642 ka and it is clear that there is no Late Quaternary palaeotopography that might have impounded a pluvial lake. If emplacement took place during a glacial (see below), a lake of unfrozen water is also unlikely. The source of the water is therefore likely to be groundwater or else ponded meltwater created during subglacial eruptions. However, eruptions involving interaction with groundwater create deposits characteristically rich in basement lithics, although the proportion can be variable (Wohletz and Sheridan 1983; Sohn 1996; White and Ross 2011). The volume of basement-derived lithics is very low in the Harrow Peaks deposits (c. 1 vol%), apart possibly from the lowest (earliest-formed) beds. This signifies that the locus of explosivity was situated at a high elevation, probably within the tephra pile, and that water was probably ponded over the vent (Sohn 1996; Pedrazzi et al. 2013). Such flooded vents are Surtseyan and the eruptive processes involve magma

mingling, steam explosivity and the incorporation of large volumes of unconsolidated waterlogged crater-filling lapilli and ash into the erupting jets (Kokelaar 1983; White 1996; Brand and Clarke 2009).

Eruption through an overlying ice sheet is capable of creating ample meltwater to drive hydrovolcanic activity, as described in models derived for other glaciovolcanic tuff cones (Smellie 2001; Schopka et al. 2006; Russell et al. 2013; Hungerford et al. 2014; Smellie and Edwards 2016). The locus of the eruption, on the saddle of a narrow-crested basement ridge, is also consistent with a subglacial eruption, where an overlying cavity or vault melted in an ice cover is required to confine the water, with heat released by the volcanic products responsible for melting the cavity. The thickness of ice that formerly overlaid the site of the tuff cone is unclear but its surface elevation was presumably above the summit of the plug, which would be needed to explain the evidence for water chilling. We thus suggest that the ice surface had a minimum elevation of c. 450 m a.s.l. (relative to present datum), i.e. c. 100 m above the inferred elevation of the vent (taking c. 350 m a.s.l. as the projected elevation of the granitoid ridge before the eruptions began). Our estimate is not well constrained and we do not take into consideration any surface sag of the ice towards the erupting vent (cf. Smellie et al. 2011b; Smellie and Edwards 2016); if such sagging did take place it would probably only add a few tens to several tens of metres to our estimate. A relatively thin ice cover is consistent with (1) the occurrence of ash-coated lapilli, indicating that a subaerial eruption column was achieved, which is unlikely under ice thicknesses of many hundreds of metres; (2) the presence of large slabs of agglutinate and unconsolidated scoria derived from the late-stage Strombolian cone that are unlikely to have subsided intact hundreds of metres into the vent; and (3) an absence of pillow lava which typically forms under thicker ice conditions (e.g. Jones 1969; Werner and Schmincke 1999; Skilling 2009; Smellie and Edwards 2016). Low vent pressures are known to favour explosive over effusive activity, including for magmas with vesicularities similar to those in the study area (cf. Gudmundsson et al. 2004; Schopka et al. 2006); an ice thickness of 100 m is equivalent to just 1 MPa and that figure will reduce if a proportion of the glacial cover was snow or firn. Zimanowski and Büttner (2003) have also argued that powerful thermohydraulic explosions are increasingly unlikely at (water) depths exceeding 100 m. Many estimates for the depth of the transition between effusive and explosive hydrovolcanic eruption for mafic magmas range between 100 and 200 m, particularly as evidenced by glaciovolcanic edifices in Iceland (e.g. Jones 1970; Allen 1980; Schopka et al. 2006). Although explosivity at greater depths is theoretically possible and has been observed rarely (e.g. Wohletz 2003; Chadwick et al. 2008; Resing et al. 2011), it is still uncertain that thermohydraulic explosivity will occur at high hydraulic pressures. On balance, a relatively thin ice cover < 100–200 m seems likely.

Thermal regime of the ice associated with the Harrow Peaks tuff cone eruptions

Determining the nature of the thermal regime of the overlying ice is important for it will control the hydraulics of the setting, which will have a major influence on the course of the eruptions (cf. Smellie 2001, 2009, 2013; Edwards et al. 2015; Smellie and Edwards 2016). Under *wet-based ice*, any subglacial vault melted in the ice will be inherently leaky (Schopka et al. 2006; Smellie 2006; Hungerford et al. 2014). If the bedrock gradient is low, the rate of basal meltwater escape will be relatively slow compared with the volume of water generated by ice melting and the meltwater will generally pond in the cavity (Smellie 2001, 2006). Conversely, if bedrock gradients are steep, such as those at the Harrow Peaks locality (c. 50–75°), their influence will dominate the hydraulic potential, causing a vault to drain continuously and preventing meltwater from accumulating (Stevenson et al. 2009). Meltwater may accumulate initially when the subglacial drainage system is relatively inefficient but thermal erosion will quickly enlarge the drainage conduits to create Röthlisberger channels (Walder 2010) and so it is unlikely that much ponded meltwater will be retained. The existence of 'dry' (i.e. drained) subglacial cavities in wet-based ice sited over steeply inclined bedrock was postulated to explain the absence of water-chilled fragmental lithofacies associated with the emplacement of intermediate-composition glaciovolcanic lava domes in British Columbia (Kelman et al. 2002; see also Stevenson et al. 2009). Thus, under wet-based ice conditions on steeply inclined bedrock, the ice cavity at Harrow Peaks would have been fully drained. An upward transition from early phreatomagmatic explosivity to 'dry' eruptions of Strombolian or Hawaiian type should occur rapidly yielding a thin basal sequence of stratified hydrovolcanic tephra overlain by a volumetrically dominant pile of magmatic tephra. A similar rapid upward progression was inferred for intermediate-composition products of eruptions beneath thin ice in 1969 at Deception Island (Antarctica; 70–100 m-thick ice; Smellie 2002); at Eyjafjallajökull, Iceland, in 2010 (c. 200 m-thick ice; Gudmundsson et al. 2012; Cioni et al. 2014); by Stevenson et al. (2011) for an Icelandic rhyolitic example; and is here inferred for Oligocene (28 Ma) mafic glaciovolcanic tuff cones erupted on steep bedrock at Mt. Petras, Antarctica, described by Wilch and McIntosh (2000). However, such a sequence is not seen at Harrow Peaks.

By contrast, *cold ice* is frozen to its bed and any meltwater created is unable to escape unless by overflowing (Smellie 2009; Smellie and Edwards 2016). Overflowing is aided by the addition of magma to the base of the vault, which displaces the

meltwater upward until it can overflow, either onto the surface directly or (usually) via a permeable surface layer such as firn, snow or fractured ice (Smellie 2006). The meltwater will accumulate until it reaches an overflow point, at which the water level is stabilised and slowly lowers due to downcutting at the spillway (cf. Raymond and Nolan 2002; Smellie 2006). Thus, for eruptions under cold ice, the resulting lithofacies should display pervasive evidence for wet conditions, becoming drier upward and with time (as the water level slowly drops).

The characteristics of the volcanic lithofacies at Harrow Peaks indicate that conditions in the tuff cone were probably water-saturated to account for the dominant sloppy-looking homogenised and deformed deposits. However, with time the deposits may have become moist rather than wet. Onset of this condition would have occurred when many of the basalt intrusions were emplaced, thus explaining their relatively coarse blocky and columnar cooling joints, and the presence of matrix vesicles in the lapilli tuffs. Matrix vesicles can occur in a low-permeability waterlogged sediment host, but their preservation requires moist conditions at sediment consolidation (Lorenz 1974). The presence of very fine grained rather than glassy margins of the intrusions is also broadly consistent with a slower cooling rate associated with emplacement in moist rather than water-saturated sediments, where the water content of the host sediment (saturated or moist) will determine the rates of heat transfer (e.g. Ratcliffe 1960; White et al. 2003).

In summary, our observations of the Harrow Peaks sequence are most easily reconciled if the tephra pile was constructed in a subglacial cavity that was melted in a cold ice glacier, in which basal drainage did not occur (i.e. it was frozen to its bed). Thus, the tephra would be waterlogged up to an overflow elevation, presumably corresponding to the lowest level of permeable firn, snow or fractured ice. Above that elevation, the pile will be moist because of water, transformed to steam by the heat of magma in the vent, condensing in the overlying pile. The overflow elevation (and hence thickness of tephra that is waterlogged) will also diminish due to thermal erosion of the overflow point. The tephra pile will thus become progressively drier upward and with time as the vent becomes isolated from the basal ponded water, culminating in 'dry' magmatic eruptions of Strombolian or Hawaiian type at a late stage. This sequence of events fits best with the preserved lithofacies at Harrow Peaks.

Volcanological and environmental implications

Construction of a tuff cone by explosive hydrovolcanic eruptions under cold-based ice

In our interpretation, the lapilli tuffs preserved at Harrow Peaks represent a proximal deposit, this probably being the

fill of a crater or ice conduit homogenised by repeated hydrovolcanic explosions. The sequence of eruptions, and evolution of the ice cover and landscape are envisaged as follows (Fig. 8):

A thin cover of cold-based ice is envisaged at c. 640 ka (Fig. 8a). The eruption was explosive at the outset and phreatomagmatic due to the interaction of magma and glacial meltwater, where explosive magma-water interaction would have produced abundant steam. Steam raised to temperatures of a few hundred degrees would have exerted overpressures of several MegaPascals, sufficient to lift and disrupt an ice cover a few hundred metres thick. Thus, we suggest that an explosively generated vertical-walled cylindrical ice conduit was created surrounded by ejecta formed of ice blocks and tephra (Fig. 8b). The Harrow Peaks deposit thus might be regarded as the fill of a diatreme bounded by ice instead of by country rocks.

Because the eruption column was largely atmospheric, proximal tephra accumulating on the surrounding ice surface would have constructed a supraglacial tuff cone edifice, or possibly a tuff ring (Fig. 8c), surrounding the ice conduit (e.g. Smellie 2002; Gudmundsson et al. 2012). Syn-eruption widening of the basal few tens of metres of the subglacial vault, caused by heat transferred to the ice cavity by warm water and tephra banked up against the ice walls, would have created an inkbottle shape to the melted cavity with a narrower tall cylindrical pathway leading to the surface (Fig. 8d). The waterlogged tephra would have undergone slumping to fill any additional space caused by melting back of the enclosing walls, expanding the width and increasing the volume of the subglacial tephra pile. Explosive events in the narrow cylindrical conduit would have thoroughly mixed the unconsolidated tephra in turbulent columns, probably ejecting some as dense water-rich jets or slurries onto the surrounding ice in addition to fall tephra, as observed in the 2004 Grímsvötn eruption (Jude-Eton et al. 2012). With explosions confined to a narrow ice-walled conduit largely filled by waterlogged tephra, it is likely that the eruption column would have been dense and relatively low, probably resulting in much material falling back into the ice conduit resulting in abundant recycling and abrasion of clasts. The repetitive explosive activity thus mixed and redeposited the accumulated tephra, destroying any stratification that may temporarily have formed within the crater, except possibly for rare relict slabs that slid in from the surrounding supraglacial cone.

By analogy with tuff cones formed in other environments, the supraglacial tuff cone flanks were probably formed of well stratified lapilli tuffs. Because they were deposited on the stable surrounding ice surface, they would have been much less disturbed by the eruptions that reworked the ice-conduit infill. Tuff cone construction would have been succeeded by the construction of a scoria cone at a late stage, probably after the vent had dried out and during the final phase of
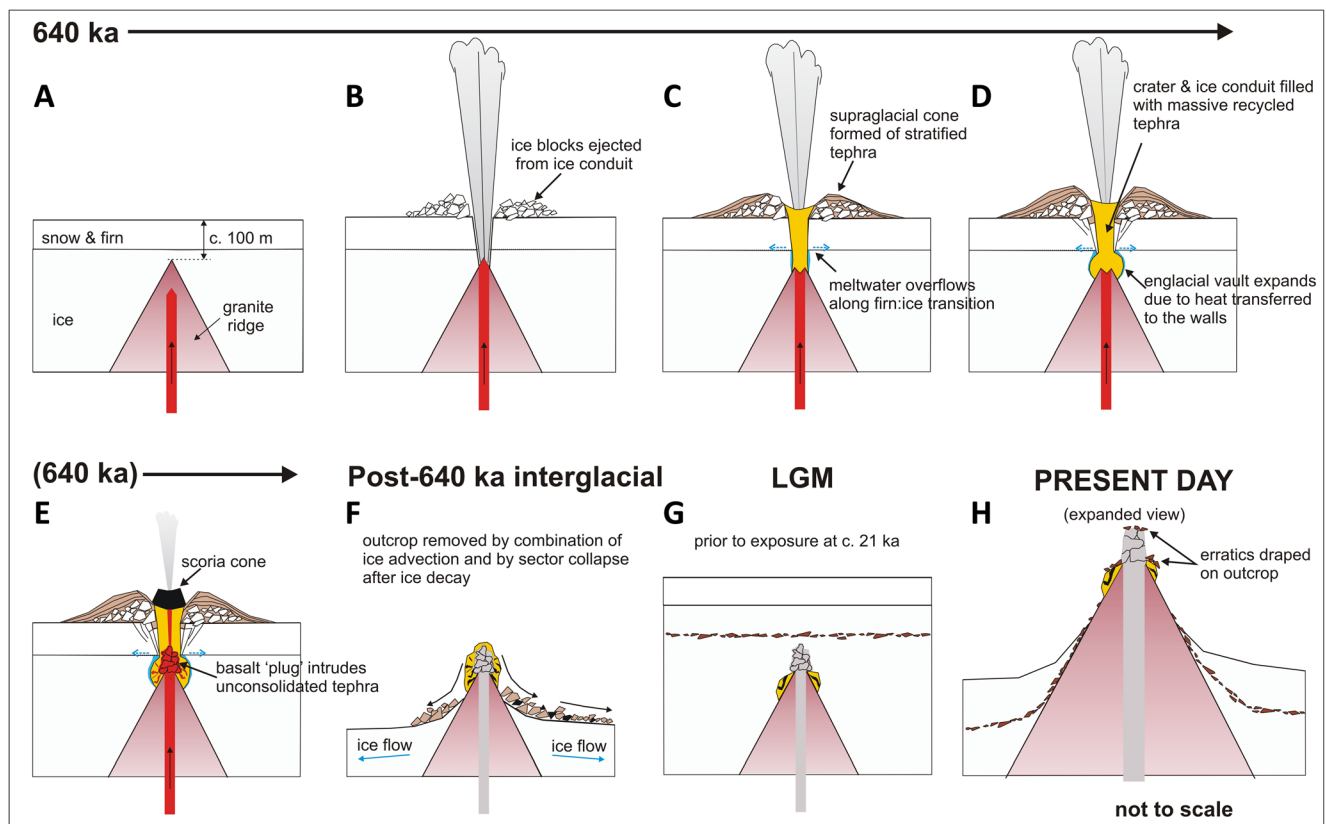
Fig. 8 Series of schematic diagrams illustrating the evolution of the Harrow Peaks tuff cone by eruption under cold-based ice. See text for description

Strombolian activity. This was followed by intrusion of a large basalt mass to form the central plug-like outcrop (Fig. 8e). Some material probably also contributed to the crater/conduit fill as the margins of the ice conduit collapsed due to the weight of accumulated tephra. This process would have been aided by heating effects that would have enlarged the base of the underlying ice cavity, undermining the ice roof and widening the ice conduit. Late-stage crater enlargement was thus probably largely by mechanical roof collapse rather than by melting of ice walls. The stratified flank deposits of the supraglacial tuff cone are not preserved at Harrow Peaks because the cone would have been advected away during subsequent ice flow, or collapsed piecemeal during ice decay in interglacials and ultimately washed away by meltwater, thus causing its complete destruction (Fig. 8f). The outcrop was subsequently covered by ice during younger glacial episodes (Fig. 8g). The outcrop was finally exposed at c. 21 ka, leaving it draped by numerous basement erratics derived from a basal dirt band advected high within the Last Glacial Maximum (LGM) ice mass (Fig. 8h).

Environmental implications

From our study of the Harrow Peaks tuff cone outcrop, we suggest that the eruption took place at 642 ± 20 ka under a cold ice cover with a minimum local surface elevation of c.

450 m a.s.l. (relative to present datum). The information available from the outcrop itself is insufficient to determine whether that ice was a substantial topography-drowning regional East Antarctic Ice Sheet, a sizeable ice dome, an icefield centred on Random Hills or simply a local ice cap within a terrain that was ice-free at lower elevations. However, the crest of the bedrock ridge underlying the tuff cone is too narrow, by itself, to sustain an ice cap ≥ 100 m thick in an otherwise ice free terrain or in an icefield setting of ridges and glaciers similar to today. In addition, the lithofacies evidence for meltwater ponded at the vent implies an ice cover that was continuous with ice at lower elevations. A regional ice sheet or substantial ice dome are thus more plausible, and consistent with an eruptive age close to the Quaternary glacial maximum corresponding to MIS16 (Fig. 10). Notably, the elevation of the ice surface during eruptions inferred by our study is considerably lower than the crest of the adjacent Random Hills (c. 1770 m a.s.l.), which suggests the presence of a broadly dome-shaped ice surface rising to the west (Fig. 9a). Because the modern glacier surfaces are a few hundred metres lower than the tuff cone outcrop, and its inferred local surface elevation of c. 450 m a.s.l. at 642 ka, the mid-Quaternary MIS16 ice sheet would have been considerably thicker than present, although not thick enough to completely drown all the topography. Since then, several glacial–interglacial cycles have taken place, including at least seven interglacials (Imbrie
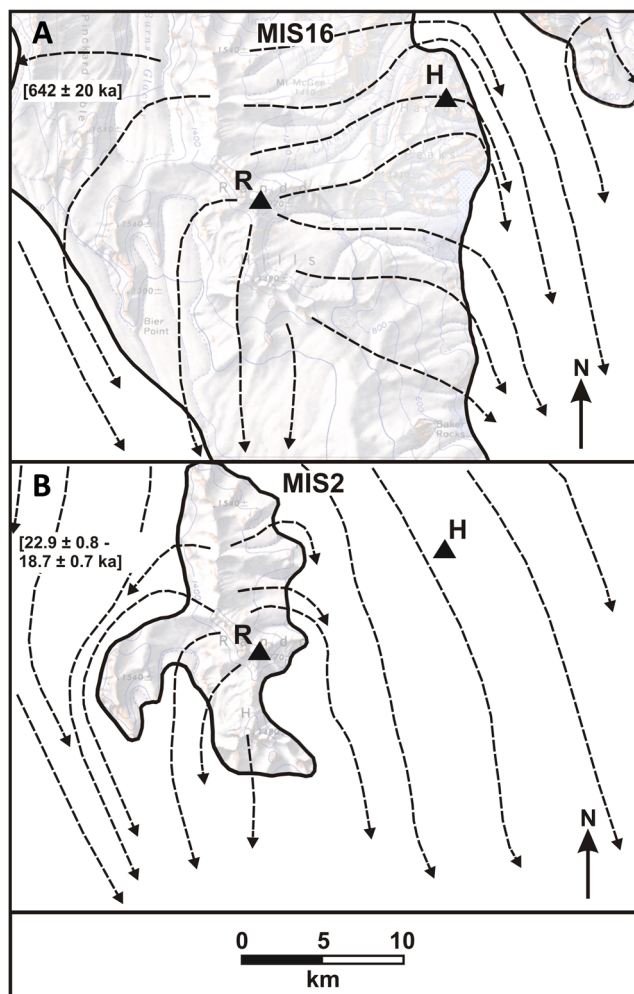
Fig. 9 Empirical reconstructions for ice surfaces during **a** MIS16 and **b** MIS2. Inferred ice domes are shown with the underlying topography faintly revealed. Because of inferred generally thinner ice during MIS16, the ice dome present then was much larger than during MIS2, leading to different ice morphologies (ice dome vs ice sheet) over the study site during the two periods. Black dashed arrows are inferred reconstructed ice flow lines. R—Random Hills summit; H—Harrow Peaks study site. Topographical base map from USGS (1967)

et al. 1984; Lang and Wolff 2011). Each interglacial presumably would have been associated with a regional ice sheet similar in appearance to today, but much thinner than that during the MIS16 glacial (Fig. 10). During the interglacial periods, the decay of the surrounding ice would have removed underlying support for the supraglacial tuff cone edifice as well as lateral buttressing support for the portion constructed subglacially. The present highly degraded appearance of the outcrop is thus not an effect of deep glacial erosion, but instead is a result of extensive collapse and removal by ice advection.

Studies of environmental change have suggested that the entire region remained in a cold ice thermal regime during the Quaternary, which should have acted predominantly to protect it (Baroni and Orombelli 1987; Orombelli et al. 1990; Baroni

et al. 2005; Di Nicola et al. 2009). However, the Harrow Peaks outcrop is draped by numerous erratics of basement granitoid lithologies that are significantly abraded (Figs. S1–S3 in Supplementary information). Although similar-looking granitoids also occur as lithic blocks in the lapilli tuffs, the latter are usually much smaller (a few decimetres across), are mainly angular–subangular, and lack the red oxidation/weathering coloration of many of the erratics. We also observed no adhering basalt or lapilli tuff matrix on any of the erratics. Together, the weight of these observations suggests that the erratics were not derived by erosion from the underlying volcanic outcrop. The abrasion observed on the erratics is also more characteristic of transport within, and deposition from, wet-based ice. However, no evidence was seen for erosion by wet-based ice on the Harrow Peaks outcrop itself (e.g. striations, polishing and other signs of ice moulding), nor are there tills or glacio-fluvial sediments. Identical relations involving abraded erratics resting on unmodified bedrock are well known in areas that were covered by cold ice in other regions of the world that experienced polythermal ice conditions (e.g. Fabel et al. 2002).

The surface exposure ages obtained on two of the erratics indicate that they were exposed at c. 20.8 ± 0.8 ka by an ice sheet significantly younger than the age of the tuff cone (Table 3). It is therefore not implicated in the formation of that tuff cone. Many of the erratic lithologies are most closely matched with Cambro–Ordovician and Cenozoic plutons exposed to the north and northwest of the study area (e.g. muscovite-bearing granite intrusions cutting the Cosmonaut Granite and small Cenozoic syenite plutons in the Mt. McGee and Styx Glacier regions; Nathan 1971; Tonarini et al. 1997; Rocchi et al. 2002). The provenance of the erratics thus suggests broadly southerly- or southeasterly-directed transport and deposition by ice. However, the rarity of syenite erratics (from parts of the Mt. McGee igneous complex; Fig. 1) suggests only minor input of erratics from the west or northwest and a southerly transport direction was probably dominant overall (Fig. 9b). Their exposure ages correspond closely to the peak of the last glacial, Marine Isotope Stage 2 (Fig. 10). They are thus reflecting ice decay associated with the LGM. A southerly flow of ice over the study site is consistent with the MIS2 ice cover over the study site being a regional ice sheet, presumably thicker and more topography-drowning than that during MIS16 when the site was beneath a major ice dome that encompassed Harrow Peaks (cf. Fig. 9a, b). By contrast, a larger ice dome during MIS2 centred over Random Hills (i.e. similar to that which we suggest for MIS16) would probably have imposed a broadly easterly ice flow at Harrow Peaks and resulted in greater numbers of syenite erratics (Fig. 9a).

Ross Sea deglaciation models suggest that grounding line retreat in the western Ross Sea passed south of Wood Bay at times varying between c. 13 and 7 ka, by which time the

Fig. 10 Diagram showing variations in $\delta^{18}O$ (after Lisiecki and Raymo 2005) for the last 800 k.y. The age of eruption of the Harrow Peaks tuff cone and two glacial erratics are also shown (data from this paper). Selected Marine Isotope Stages are also numbered
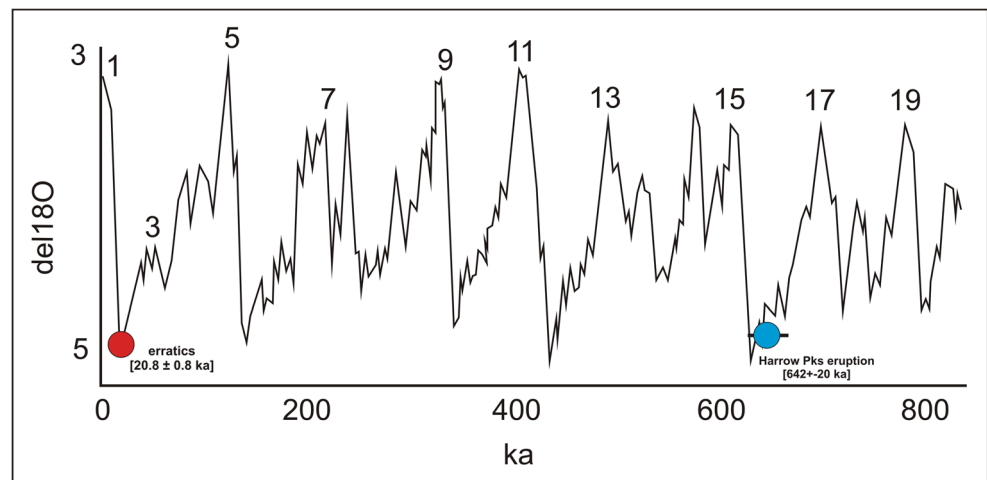
coastal ice morphology, surface gradients and surface elevations were probably broadly similar to today (e.g. Denton and Hughes 2002; Anderson et al. 2014; Halberstadt et al. 2016). Exposure of the bedrock ridges at Harrow Peaks took place only a few thousand years prior to the timing of grounding line retreating to the south of Wood Bay. This suggests that the Harrow Peaks ridges were exposed by the decaying ice relatively quickly once peak glacial conditions had passed, and that the coeval ice sheet either decayed quite rapidly or else it was relatively thin above the volcanic outcrop, although at least several hundred metres thicker than today in the Random Hills–Harrow Peaks area. This is broadly consistent with some published syntheses of ice sheet thicknesses, which are inferred to have been more than 360 m to more than 700 m thick around coastal East Antarctica (Mackintosh et al. 2014). Under such conditions, the higher topography of Random Hills might still have formed a small local ice dome but it was unable to deflect ice flow across Harrow Peaks, which were fully submerged by the regional ice cover (Fig. 9b).

Finally, despite the presence of abraded erratics at Harrow Peaks, the volcanic outcrop lacks evidence for wet-based ice erosion, implying that the overlying ice at LGM was cold-based. These conflicting observations can be resolved if the overall thermal regime of regional ice in coastal Victoria Land was polythermal, i.e. a geographically complicated patchwork mosaic of cold-based and wet-based ice, perhaps with cold ice on summits and ridges and wet-based ice below thicker ice in valley bottoms, although natural systems are likely to be more complicated (e.g. Fabel et al. 2002). Thus, we suggest that plucking and abrasion of the erratics was initially caused by patches of erosive wet-based ice in the Victoria Land hinterland broadly to the north of Harrow Peaks, and the debris was transferred into cold-based ice during southerly transport, possibly by thrusting and internal deformation at the boundaries between wet-and cold-based ice masses (cf. Hambrey and Glasser 2012). The erratics were finally released by a decaying ice sheet that was cold-based over the study site at

Harrow Peaks. This scenario is similar to the thermal state envisaged for late Miocene and Pliocene ice in northern Victoria Land (Smellie et al. 2014), and by modelling studies of the modern Antarctic ice sheet in East Antarctica (Pollard and De Conto 2009; Pattyn 2010). Erratics showing similar edge abrasion and surface oxidation/weathering are common in the region and are known as Terra Nova Drift (Baroni and Orombelli 1987; Orombelli et al. 1990; Di Nicola et al. 2009). Similarly abraded erratics exposed at c. 16 ka are also present at Cape Adare at 350 m a.s.l., c. 400 km to the north (Johnson et al. 2008). The distribution of the abraded erratics described in this paper and by other authors (e.g. Baroni and Orombelli 1987; Orombelli et al. 1990; Di Nicola et al. 2009) may suggest that polythermal ice had a widespread distribution in the Mt. Melbourne hinterland during the last glacial, and potentially extended along 400 km of coastal Victoria Land (Harrow Peaks–Cape Adare), at least.

Conclusions

The remains of a volcanic centre at Harrow Peaks (Victoria Land, Antarctica) are interpreted as a small monogenetic tuff cone formed by a hydrovolcanic (phreatomagmatic) eruption of basanite–hawaiite magma at 642 ± 20 ka. The outcrop is deeply degraded, its mafic plug-filled core is exposed and it is strewn with abundant abraded basement erratics. However, the outcrop is not glacially eroded, despite being erupted close to the peak of the MIS16 glacial. From interpretation of the lithofacies and likely eruptive mechanisms, the weight of the evidence suggests that the eruptions took place under a relatively thin ice sheet that was cold-based rather than wet-based. If true, the outcrop thus represents the anatomy of a tuff cone erupted under cold (frozen-bed) ice. The most important distinguishing feature compared with tuff cones erupted in other environmental settings is the overwhelming dominance of massive lapilli tuff rich in fine ash matrix and abraded

lapilli. The scarcity of stratification is probably due to its destruction during repeated eruption through a cylindrical cavity (analogous to an ice-walled diatreme) blasted through a thin ice cover that was probably 100–200 m thick over the vent. The deposit is thus thought to correspond mainly to an ice conduit infill linked to a supraglacial tuff cone. The coeval ice for the Harrow Hills outcrop probably formed a substantial dome centred over Random Hills. The bulk of the tuff cone was constructed mainly on the surrounding ice surface where it was subsequently removed by ice advection or destroyed by the ice as it ultimately decayed and removed support by buttressing, thus causing extensive sector collapse. Dating by ^{10}Be cosmogenic nuclide exposure of associated granitoid basement erratics indicates that the volcanic outcrop was most recently exposed by decay of locally cold-based ice at c. 20.8 ± 0.8 ka (MIS2). The coeval ice was part of a regional ice sheet that was thicker than that at 642 ka. Despite the prominent abrasion shown by the erratics, no glacial erosion of the underlying volcanic outcrop is evident, and the local MIS2 ice was probably cold-based but within a regional basal thermal regime for the ice that was polythermal overall, similar to the Miocene–Pliocene setting.

References

Allen CC (1980) Icelandic subglacial volcanism: thermal and physical studies. J Geol 88(1):108–117. https://doi.org/10.1086/628478

Anderson JB, Conway H, Bart PJ, Witus AE, Greenwood SL, McKay RM, Hall BL, Ackert RP, Licht K, Jakobsson M, Stone JO (2014) Ross Sea paleo-ice sheet drainage and deglacial history during and since the LGM. Quat Sci Rev 100:31–54. https://doi.org/10.1016/j.quascirev.2013.08.020

Armienti P, Civetta L, Innocenti F, Manetti P, Tripodo A, Villari L, Vita G (1991) New petrological and geochemical data on Mt. Melbourne volcanic field, northern Victoria Land, Antarctica. (II Italian Antarctic expedition). Mem Soc Geol Ital 46:397–424

Balco G (2011) Contributions and unrealized potential contributions of cosmogenic-nuclide exposure dating to glacier chronology, 1990-2010. Quat Sci Rev 30(1-2):3–27. https://doi.org/10.1016/j.quascirev.2010.11.003

Baroni C, Orombelli G (1987) Glacial geology and geomorphology of Terra Nova Bay (Victoria Land, Antarctica). Mem Soc Geol Ital 33: 171–193

Baroni C, Noti V, Ciccacci S, Righini G, Salvatore MC (2005) Fluvial origin of the valley system in northern Vitoria Land (Antarctica) from quantitative geomorphic analysis. Geol Soc Am Bull 117(1): 212–228. https://doi.org/10.1130/B25529.1

Benn DI, Evans DJA (1998) Glaciers and glaciation. Arnold, London 734 pp

Bennett MR, Huddart D, Gonzalez S (2009) Glaciovolcanic landsystem and large-scale glaciotectonic deformation along the Brekknafjöll—Jarlhettur, Iceland. Quat Sci Rev 28: 647–676

Brand BD, Clarke AB (2009) The architecture, eruptive history, and evolution of the table rock complex, Oregon: from a Surtseyan to an energetic maar eruption. J Volcanol Geotherm Res 180(2-4):203–224. https://doi.org/10.1016/j.jvolgeores.2008.10.011

Branney MJ, Kokelaar P (2002) Pyroclastic density currents and the sedimentation of ignimbrites. Geol Soc Lond Mem 27:143

Brown RJ, Bonadonna C, Durant AJ (2012) A review of volcanic ash aggregation. Phys Chem Earth 45-46:65–78. https://doi.org/10.1016/j.pce.2011.11.001

Carmignani L, Ghezzo C, Gosso G, Lombardo B, Meccheri M, Perusati PC, Salvini F (1988) Geological map of the area between David and Mariner Glaciers, Victoria Land (Antarctica). PNRA-CNR-ENEA, Firenze, Litografia artistica cartografica. Mem Soc Geol It 33

Chadwick WW, Cashman KV, Embley RW, et al (2008) Direct video and hydrophone observations of submarine explosive eruptions at NW Rota-1 volcano, Mariana arc. J Geophys Res 113:article B08S10

Cioni R, Pistolesi M, Bertagini A, Bonadonna C, Höskuldsson A, Scateni B (2014) Insights into the dynamics and evolution of the 2010 Eyjafjallajökull summit eruption (Iceland) provided by volcanic ash textures. Earth Planet Sci Lett 394:111–123. https://doi.org/10.1016/j.epsl.2014.02.051

Cole PD, Guest JE, Duncan AM, Pacheco J-M (2001) Capelinhos 1957-1958, Faial, Azores: deposits formed by an emergent surtseyan eruption. Bull Volcanol 63(2-3):204–220. https://doi.org/10.1007/s004450100136

D'Oriano C, Bertagnini A, Cioni R, Pompilio M (2014) Identifying recycled ash in basaltic eruptions. Nature Sci Reps 4(1): doi: https://doi.org/10.1038/srep05851,

Denton GH, Hughes TJ (2002) Reconstructing the Antarctic ice sheet at the last glacial maximum. Quat Sci Rev 21(1-3):193–202. https://doi.org/10.1016/S0277-3791(01)00090-7

Di Nicola L, Strasky S, Schlüchter C, Salvatore MC, Akçar N, Kubik PW, Christl M, Kasper HU, Wieler R, Baroni C (2009) Multiple cosmogenic nuclides document complex Pleistocene exposure history of glacial drifts in Terra Nova Bay (northern Victoria Land, Antarctica). Quat Res 71(01):83–92. https://doi.org/10.1016/j.yqres.2008.07.004

Di Vincenzo G, Bracciali L, Del Carlo P, Panter K, Rocchi S (2010) 40Ar–39Ar dating of volcanogenic products 1 from the AND-2A core (ANDRILL Southern McMurdo Sound Project, Antarctica): correlations with the Erebus Volcanic Province and implications for the age model of the core. Bull Volcanol 72: 487–505

Edwards BR, Russell JK (2002) Glacial influences on morphology and eruptive products of Hoodoo Mountain volcano, Canada. In: Smellie JL, Chapman MG (eds) Volcano–ice interaction on earth and Mars. Geol Soc Lond Spec Publ 202(1): pp. 179–194. doi: https://doi.org/10.1144/GSL.SP.2002.202.01.09

Edwards BR, Russell JK, Gudmundsson MT (2015) Glaciovolcanism. In: Sigurdsson H, Houghton B, Rymer H, Stix J, McNutt S (eds) The

encyclopedia of volcanoes, 2nd edn. Academic Press, San Diego, pp 377–393. https://doi.org/10.1016/B978-0-12-385938-9.00020-1

Fabel D, Stroeven AP, Harbor J, Kleman J, Elmore D, Fink D (2002) Landscape preservation under Fennoscandian ice sheets determined from in situ produced ^{10}Be and ^{26}Al. Earth Planet Sc Lett 201(2): 397–406. https://doi.org/10.1016/S0012-821X(02)00714-8

Giordano G, Lucci F, Phillips D, Cozzupoli D, Runci V (2012) Stratigraphy, geochronology and evolution of the Mt. Melbourne volcanic field (North Victoria land, Antarctica). Bull Volcanol 74(9):1985–2005. https://doi.org/10.1007/s00445-012-0643-8

Gudmundsson MT, Sigmundsson F, Björnsson H, Högnadóttir TH (2004) The 1996 eruption at Gjálp, Vatnajökull icecap, Iceland: efficiency of heat transfer, ice deformation and subglacial water pressure. Bull Volcanol 66(1):46–65. https://doi.org/10.1007/s00445-003-0295-9

Gudmundsson MT, Thordarson T, Höskuldsson Á, Larsen G, Björnsson H, Prata AJ, Oddsson B, Magnússon E, Högnadóttir T, Pedersen GN, Hayward CL, Stevenson JA, Jónsdóttir I (2012) Ash generation and distribution from the April-May 2010 eruption of Eyjafjallajökull, Iceland. Nat Sci Rep 2(1):572. https://doi.org/10.1038/srep00572.

Halberstadt AR, Simkins LM, Grenwood SL, Anderson JB (2016) Past ice-sheet behaviour: retreat scenarios and changing controls in the Ross Sea, Antarctica. Cryosphere 10(3):1003–1020. https://doi.org/10.5194/tc-10-1003-2016

Hambrey MJ, Glasser NF (2012) Discriminating glacier thermal and dynamic regimes in the sedimentary record. Sed Geol 251-252:1–33. https://doi.org/10.1016/j.sedgeo.2012.01.008

Houghton BF, Smith RT (1993) Recycling of magmatic clasts during explosive eruptions: estimating the true juvenile content of phreatomagmatic volcanic deposits. Bull Volcanol 55(6):414–420. https://doi.org/10.1007/BF00302001

Houghton BF, Wilson CJN (1989) A vesicularity index for pyroclastic deposits. Bull Volcanol 51(6):451–462. https://doi.org/10.1007/BF01078811

Hungerford JDG, Edwards BR, Skilling IP, Cameron B (2014) Evolution of a subglacial basaltic lava flow field: Tennena volcanic center, Mount Edziza volcanic complex, British Columbia, Canada. J Volcanol Geotherm Res 272:39–58. https://doi.org/10.1016/j.jvolgeores.2013.09.012

Imbrie J, Hays JD, Martinson DG, McIntyre A, Mix AC, et al (1984) The orbital theory of Pleistocene climate: support from a revised chronology of the marine δ18O record. In: Berger AL, Imbrie J, Hays JD, Kukla G, Saltzman B. (eds) Milankovitch and Climate (Pt. I): Dordrecht (Reidel), pp. 269–305

IPCC (2013) Climate change 2013: the physical science basis. Contribution of working group I to the fifth assessment report of the intergovernmental panel on climate change [Stocker, T.F., D. Qin, G.-K. Plattner, M. Tignor, S.K. Allen, J. Boschung, A. Nauels, Y. Xia, V. Bex and P.M. Midgley (eds)]. Cambridge University Press, Cambridge, UK and New York, USA, 1535 pp

Johnson JS, Hillenbrand C-D, Smellie JL, Rocchi S (2008) The last deglaciation of cape Adare, northern Victoria Land, Antarctica. Ant Sci 20(06):581–587. https://doi.org/10.1017/S0954102008001417

Jones JG (1969) Intraglacial volcanoes of the Laugarvatn region, southwest Iceland—I. Quart J Geol Soc Lond 124:197–211

Jones JG (1970) Intraglacial volcanoes of the Laugarvatn region, southwest Iceland II. J Geol 78(2):127–140. https://doi.org/10.1086/627496

Jude-Eton TC, Thordarson T, Gudmundsson MT, Oddsson B (2012) Dynamics, stratigraphy and proximal dispersal of supraglacial tephra during the ice-confined 2004 eruption of Grímsvötn volcano, Iceland. Bull Volcanol 74(5):1057–1082. https://doi.org/10.1007/s00445-012-0583-3

Kelman MC, Russell JK, Hickson CJ (2002) Effusive intermediate glaciovolcanism in the garibaldi Volcanic Belt, southwestern British Columbia, Canada. In: Smellie JL, chapman MG (eds) Volcano–ice interaction on Earth and Mars. Geol Soc Lond Spec Publ 202(1):195–211. doi:https://doi.org/10.1144/GSL.SP.2002.202.01.10

Kokelaar BP (1983) The mechanism of Surtseyan volcanism. J Geol Soc Lond 140(6):939–944. https://doi.org/10.1144/gsjgs.140.6.0939

Lang N, Wolff EW (2011) Interglacial and glacial variability from the last 800 ka in marine, ice and terrestrial archives. Clim Past 7(2):361–380. https://doi.org/10.5194/cp-7-361-2011

Lisiecki LE, Raymo ME (2005) A Pliocene-Pleistocene stack of 57 globally distributed benthic δ^{18}O records. Paleoceanography 20: PA 1003. doi:https://doi.org/10.1029/2004PA001071

Long PE, Wood BJ (1986) Structures, textures and cooling histories of Columbia River basalt flows. Geol Soc Am Bull 97(9):1144–1155. https://doi.org/10.1130/0016-7606(1986)97<1144:STACHO>2.0.CO;2

Lorenz V (1974) Vesiculated tuffs and associated features. Sedimentology 21(2):273–291. https://doi.org/10.1111/j.1365-3091.1974.tb02059.x

Lyon GL (1986) Stable isotope stratigraphy of ice cores and the age of the last eruption at Mount Melbourne, Antarctica. N Z J Geol Geophys 29(1):135–138. https://doi.org/10.1080/00288306.1986.10427528

Mackintosh AN, Verleyen E, O'Brien PE, and 21 authors (2014) Retreat history of the East Antarctic ice sheet since the last glacial maximum. Quat Sci Rev 100: 10–30, DOI: https://doi.org/10.1016/j.quascirev.2013.07.024

Manga M, Patel A, Dufek J (2011) Rounding of pumice clasts during transport: field measurements and laboratory studies. Bull Volcanol 73(3):321–333. https://doi.org/10.1007/s00445-010-0411-6

McGarvie DW, Stevenson JA, Burgess T, Tuffen H, Tindle AG (2007) Volcano–ice interactions at Prestahnúkur, Iceland: rhyolite eruption during the last interglacial–glacial transition. In: Clarke G, Smellie J (eds) Papers from the international symposium on earth and planetary ice–volcano interactions held in Reykjavik, Iceland, on 19–23 June, 2006. An Glaciol 45: pp. 38–47

Moore JG (1985) Structure and eruptive mechanisms at Surtsey Volcano, Iceland. Geol Mag 122: 649–661

Mulder T, Alexander J (2001) The physical character of subaqueous sedimentary density flows and their deposits. Sedimentology 48(2):269–299. https://doi.org/10.1046/j.1365-3091.2001.00360.x

Nathan S (1971) Geology and petrology of the Campbell–Aviator divide, northern Victoria Land, Antarctica. Part 2—Paleozoic and Precambrian rocks. N Z J Geol Geophys 14(3):564–596. https://doi.org/10.1080/00288306.1971.10421948

Orombelli G, Baroni C, Denton GH (1990) Late Cenozoic glacial history of the Terra Nova Bay region, northern Victoria Land, Antarctica. Geogr Fis E Din Quat 13:139–163

Pattyn F (2010) Antarctic subglacial conditions inferred from a hybrid ice sheet/ice stream model. Earth Planet Sci Lett 295(3-4):451–461. https://doi.org/10.1016/j.epsl.2010.04.025

Pedrazzi D, Martí J, Geyer A (2013) Stratigraphy, sedimentology and eruptive mechanisms in the tuff cone of el Golfo (Lanzarote, Canary Islands). Bull Volcanol 75(7):740. https://doi.org/10.1007/s00445-013-0740-3

Pollard D, De Conto RM (2009) Modelling West Antarctic ice sheet growth and collapse through the past five million years. Nature 458(7236):329–332. https://doi.org/10.1038/nature07809

Putnam AE, Denton GH, Schaefer JM, Barrell DJA, Andersen BG, Finkel RC, Schwartz R, Doughty AM, Kaplan MR, Schlüchter C (2010) In situ cosmogenic ^{10}Be production-rate calibration from the Southern Alps, New Zealand. Quat Geochron 5(4):392–409. https://doi.org/10.1016/j.quageo.2009.12.001

Ratcliffe EH (1960) The thermal conductivity of ocean sediments. J Geophys Res 65(5):1535–1541. https://doi.org/10.1029/JZ065i005p01535

Raymond CF, Nolan M (2002) Drainage of a glacial lake through an ice spillway. IAHS Publ 264:199–207

Resing JA, Rubin KH, Embley RW, Lupton JE, Baker ET, Dziak RP, Baumberger T, Lilley MD, Huber JA, Shank TM, Butterfield DA, Clague DA, Keller NS, Merle SG, Buck NJ, Michael PJ, Soule A, Caress DW, Walker SL, Davis R, Cowen JP, Reysenbach AL, Thomas H (2011) Active submarine eruption of boninite in the northeastern Lau Basin. Nat Geosci 4(11):799–806. https://doi.org/10.1038/ngeo1275

Rocchi S, Tonarini S, Armienti P, Innocenti F, Manetti P (1998) Geochemical and isotopic structure of the early Palaeozoic active margin of Gondwana in northern Victoria Land, Antarctica. Tectonophysics 284(3-4):261–281. https://doi.org/10.1016/S0040-1951(97)00178-9

Rocchi S, Armienti P, D'Orazio M, Tonarini S, Wijbrans J, Di Vincenzo G (2002) Cenozoic magmatism in the western Ross Embayment: role of mantle plume vs. plate dynamics in the development of the West Antarctic Rift System. J Geophys Res 107(B9):2195. https://doi.org/10.1029/2001JB000515

Rocchi S, Bracciali L, Di Vincenzo G, Gemelli M, Ghezzo C (2011) Arc accretion to the early Paleozoic Antarctic margin of Gondwana in Victoria land. Gondwana Res 19(3):594–607. https://doi.org/10.1016/j.gr.2010.08.001

Rose WI, Durant AJ (2009) Fine ash content of explosive eruptions. J Volcanol Geotherm Res 186(1-2):32–39. https://doi.org/10.1016/j.jvolgeores.2009.01.010

Russell JL, Edwards BR, Poritt LA (2013) Pyroclastic passage zones in glaciovolcanic sequences. Nat Comm 4:1788. https://doi.org/10.1038/ncomms2829

Sæmundsson K (1970) Interglacial lava flows in the lowlands of southern Iceland and the problem of two-tiered columnar jointing. Jökull 20: 62–77

Salvini F, Brancolini G, Busetti M, Storti F, Mazzarini F, Coren F (1997) Cenozoic geodynamics of the Ross Sea region, Antarctica: crustal extension, intraplate strike-slip faulting, and tectonic inheritance. J Geophys Res 102(B11):24669–624696. https://doi.org/10.1029/97JB01643

Schaefer JM, Denton GH, Kaplan M, Putnam A, Finkel RC, Barrell DJ, Andersen BG, Schwartz R, Mackintosh A, Chinn T, Schlüchter C (2009) High-frequency Holocene glacier fluctuations in New Zealand differ from the northern signature. Science 324(5927): 622–625. https://doi.org/10.1126/science.1169312

Schopka HH, Gudmundsson MT, Tuffen H (2006) The formation of Helgafell, southwest Iceland, a monogenetic subglacial hyaloclastite ridge: sedimentology, hydrology and volcano-ice interaction. Bull Volcanol 152:359–377

Skilling IP (2009) Subglacial to emergent basaltic volcanism at Hlöðufell, southwest Iceland: a history of ice-confinement. J Volcanol Geotherm Res 186:276–289

Smellie JL (2001) Lithofacies architecture and construction of volcanoes erupted in englacial lakes: icefall Nunatak, Mount Murphy, eastern Marie Byrd Land, Antarctica. In: White JDL, Riggs N (eds) Volcaniclastic sedimentation in lacustrine settings. Intl Assoc Sedimentol Spec Publ 30: pp. 9–34. doi:https://doi.org/10.1002/9781444304251.ch2

Smellie JL (2002) The 1969 subglacial eruption on Deception Island (Antarctica): events and processes during an eruption beneath a thin glacier and implications for volcanic hazards. In: Smellie JL, chapman MG (eds) Volcano–ice interaction on Earth and Mars. Geol Soc Lond Spec Publ 202(1): pp. 59–79. doi:https://doi.org/10.1144/GSL.SP.2002.202.01.04

Smellie JL (2006) The relative importance of supraglacial versus subglacial meltwater escape in basaltic subglacial tuya eruptions: an important unresolved conundrum. E-Sci Rev 74:241–268

Smellie JL (2009) Terrestrial sub-ice volcanism: landform morphology, sequence characteristics and environmental influences, and implications for candidate Mars examples. In: Chapman MG, Leszthely L (eds.) Preservation of random mega-scale events on Mars and Earth: influence on geologic history. Geol Soc Am Spec Pap 453: pp. 55–76

Smellie JL (2013) Quaternary vulcanism: subglacial landforms. In: Elias SA (ed) The encyclopedia of quaternary science, vol 1, 2nd edn. Elsevier, Amsterdam, pp 780–802. https://doi.org/10.1016/B978-0-444-53643-3.00074-1

Smellie JL (In press). Glaciovolcanism—a 21st century proxy for palaeo-ice. In: Menzies J van der Meer J (eds) Past glacial environments (sediments, forms and techniques). Elsevier

Smellie JL, Edwards BR (2016) Glaciovolcanism on Earth and Mars. Products, processes and palaeoenvironmental significance. Cambridge University Press, Cambridge, p 483

Smellie JL, Skilling IP (1994) Products of subglacial eruptions under different ice thicknesses: two examples from Antarctica. Sediment Geol 91(1-4):115–129. https://doi.org/10.1016/0037-0738(94)90125-2

Smellie JL, Johnson JS, McIntosh WC, Esser R, Gudmundsson MT, Hambrey MJ, van Wyk de Vries B (2008) Six million years of glacial history recorded in volcanic lithofacies of the James Ross Island volcanic group, Antarctic Peninsula. Palaeogeogr Palaeoclimatol Palaeoecol 260(1-2):122–148. https://doi.org/10.1016/j.palaeo.2007.08.011

Smellie JL, Haywood AM, Hillenbrand C-D, Lunt DJ, Valdes PJ (2009) Nature of the Antarctic Peninsula Ice Sheet during the Pliocene: geological evidence & modelling results compared. E-Sc Rev 94: 79–94

Smellie JL, Rocchi S, Armienti P (2011a) Late Miocene volcanic sequences in northern Victoria Land, Antarctica: products of glaciovolcanic eruptions under different thermal regimes. Bull Volcanol 73(1):1–25. https://doi.org/10.1007/s00445-010-0399-y

Smellie JL, Rocchi S, Gemelli M, Di Vincenzo G, Armienti P (2011b) Late Miocene East Antarctic ice sheet characteristics deduced from terrestrial glaciovolcanic sequences in northern Victoria Land, Antarctica. Palaeogeogr Palaeoclimatol Palaeoecol 307(1-4):129–149. https://doi.org/10.1016/j.palaeo.2011.05.008

Smellie JL, Rocchi S, Wilch TI, Gemelli M, Di Vincenzo G, McIntosh W, Dunbar N, Panter K, Fargo A (2014) Glaciovolcanic evidence for a polythermal Neogene East Antarctic ice sheet. Geology 42(1):39–41. https://doi.org/10.1130/G34787.1

Smellie JL, Walker AJ, McGarvie DW, Burgess R (2016) Complex circular subsidence structures in tephra deposited on large blocks of ice: Varða tuff cone, Öræfajökull, Iceland. Bull Volcanol 78(8):56. https://doi.org/10.1007/s00445-016-1048-x

Sohn YK (1996) Hydrovolcanic processes forming basaltic tuff rings and cones on Cheju Island, Korea. Bull Volcanol 108:1199–1211

Sohn YK, Cronin SJ, Brenna M, Smith IEM, Németh K, White JDL, Murtagh RM, Jeon YM, Kwon CW (2012) Ilchulbong tuff cone, Jeju Island, Korea, revisited: a compound monogenetic volcano involving multiple magma pulses, shifting vents, and discrete eruptive phases. Geol Soc Am Bull 124(3-4):259–274. https://doi.org/10.1130/B30447.1

Solgevik H, Mattsson HB, Hermelin O (2007) Growth of an emergent tuff cone: fragmentation and depositional processes recorded in the Capelas tuff cone, São Miguel, Azores. J Volcanol Geotherm Res 159(1-3):246–266. https://doi.org/10.1016/j.jvolgeores.2006.06.020

Stevenson JA, Smellie JL, McGarvie DW, Gilbert JS, Cameron BI (2009) Subglacial intermediate volcanism at Kerlingarfjöll, Iceland:

magma–water interactions beneath thick ice. J Volcanol Geotherm Res 185(4):337–351. https://doi.org/10.1016/j.jvolgeores.2008.12.016

Stevenson JA, Gilbert JS, McGarvie DW, Smellie JL (2011) Explosive rhyolite tuya formation: classic examples from Kerlingarfjöll, Iceland. Quat Sci Rev 30(1-2):192–209. https://doi.org/10.1016/j.quascirev.2010.10.011

Stump E (1995) The Ross Orogen of the Transantarctic Mountains. Cambridge University Press, Cambridge 284 pp

Tonarini S, Rocchi S, Armienti P, Innocenti F (1997) Constraints on timing of Ross Sea rifting inferred from Cainozoic intrusions from northern Victoria Land, Antarctica. In: Ricci CA (ed.) The Antarctic Region: Geological Evolution and Processes. Proc VII Intl Symp Antarct E Sci, Siena, 1995. Siena, pp. 511–521

USGS (1967) Mount Melbourne, Antarctica. Topographical map SS 58-60/9. USGS 1:250 000 scale reconnaissance series. United States Geological Survey & National Science Foundation

Valentine GA, White JDL (2012) Revised conceptual model for maar-diatremes: subsurface processes, energetics, and eruptive products. Geology 40(12):1111–1114. https://doi.org/10.1130/G33411.1

Verwoerd WJ, Chevalier L (1987) Contrasting types of surtseyan tuff cones on Marion and Prince Edward islands, southwest Indian Ocean. Bull Volcanol 49(1):399–417. https://doi.org/10.1007/BF01046633

Walder JS (2010) Röthlisberger channel theory: its origins and consequences. J Glaciol 56(200):1079–1086. https://doi.org/10.3189/002214311796406031

Walker GPL (1984) Characteristics of dune-bedded pyroclastic surge. J Volcanol Geotherm Res 20(3-4):281–296. https://doi.org/10.1016/0377-0273(84)90044-1

Werner R, Schmincke H-U (1999) Englacial versus lacustrine origin of volcanic table mountains: evidence from Iceland. Bull Volcanol 60(5):335–354. https://doi.org/10.1007/s004450050237

White JDL (1996) Pre-emergent construction of a lacustrine basaltic volcano, Pahvant Butte, Utah (USA). Bull Volcanol 58(4):249–262. https://doi.org/10.1007/s004450050138

White JDL, Houghton BF (2006) Primary volcaniclastic rocks. Geology 34(8):677–680. https://doi.org/10.1130/G22346.1

White JDL, Ross P-S (2011) Maar-diatreme volcanoes: a review. J Volcanol Geotherm Res 201(1-4):1–29. https://doi.org/10.1016/j.jvolgeores.2011.01.010

White JDL, Smellie JL, Clague D (2003) Introduction: a deductive outline and topical overview of subaqueous explosive volcanism. In: White JDL, Smellie JL, Clague D (eds) Am Geophys Union Geophys Monogr 140: 1–23

Wilch TI, McIntosh WC (2000) Eocene and Oligocene volcanism at Mount Petras, Marie Byrd Land: implications for middle Cenozoic ice sheet reconstructions in West Antarctica. Ant Sci 12:477–491

Wohletz KH (2003) Water/magma interaction: physical considerations for the deep submarine environment. In White JDL, Smellie JL, Clague D (eds) Am Geophys Union Geophys Monogr 140: 25–49

Wohletz KH, Sheridan MF (1983) Hydrovolcanic explosions II. Evolution of basaltic tuff rings and tuff cones. Am J Sci 283(5): 385–413. https://doi.org/10.2475/ajs.283.5.385

Wörner G, Viereck L (1987) Subglacial to emergent volcanism at Shield Nunatak, Mt. Melbourne volcanic field, Antarctica. Polarforsch 57: 27–41

Wörner G, Viereck L, Hertogen J, Niephaus H (1989) The Mt. Melbourne field (Victoria Land, Antarctica) II. Geochemistry and magma genesis. Geol Jahrb E38:395–433

Zimanowski B, Büttner R (2003) Phreatomagmatic explosions in subaqueous volcanism. In: White JDL, Smellie JL, Clague D (eds) Am Geophys Union Geophys Monogr 140: 51–60